

## THE OUTER SOLAR SYSTEM FOR 200 MILLION YEARS

JAMES H. APPLGATE

Department of Astronomy, Columbia University, New York, New York 10027

MICHAEL R. DOUGLAS

Department of Physics, California Institute of Technology, Pasadena, California 91125

YEKTA GÜRSEL

The Artificial Intelligence Laboratory, Massachusetts Institute of Technology, Cambridge, Massachusetts 02139

GERALD J. SUSSMAN

Department of Electrical Engineering and Computer Science, and The Artificial Intelligence Laboratory, Massachusetts Institute of Technology, Cambridge, Massachusetts 02139

JACK WISDOM

Department of Earth, Atmospheric, and Planetary Sciences, Massachusetts Institute of Technology, Cambridge, Massachusetts 02139

*Received 25 September 1985; revised 19 March 1986*

## ABSTRACT

We have used a special-purpose computer to integrate the orbits of the outer five planets for more than 100 Myr into the future and more than 100 Myr into the past. The strongest features in the Fourier transforms of the orbital elements of the Jovian planets can be identified with the frequencies predicted by linear secular theory. Many of the weaker features in the Fourier spectra are identified as linear combinations of the basic frequencies. We note serious differences between our measurements and the predictions of Bretagnon (1974). The amplitude of the 3.796 Myr period libration of Pluto's longitude of perihelion is modulated with a period of 34 Myr. Very long periods, on the order of 137 Myr, are also seen. The orbit of Pluto is stable for the duration of our integration; the maximum Lyapunov characteristic exponent is less than  $10^{-6.8} \text{ yr}^{-1}$ .

## INTRODUCTION

The determination of the stability of the solar system is one of the oldest problems in astronomy, but despite considerable attention, there is no proof of the stability of the system. Systems with two degrees of freedom which are coupled sufficiently weakly have been shown to be stable for all time by the Kolmogorov-Arnold-Moser (KAM) theorem; the stability of the solar system has been demonstrated under the conditions that the masses of the planets, their eccentricities, and their inclinations are sufficiently small (Arnold 1961). The actual solar system, however, does not meet the stringent requirements of the KAM theorem. Certainly, the great age of the solar system demands a high level of stability, but weak instabilities may still be present. Wisdom (1982, 1983) has shown that planetary systems which appear to be stable may in fact be slightly unstable (have a small positive Lyapunov characteristic exponent), and that this slight instability can manifest itself in dramatic and relatively sudden changes in an orbit. The stability of the solar system should thus not be taken for granted.

Pluto's orbit is unique among the planets. It is both highly eccentric ( $e \approx 0.25$ ) and highly inclined ( $i \approx 16^\circ$ ). The orbits of Pluto and Neptune cross one another, a condition permitted only by the libration of a resonant argument associated with the  $3/2$  mean-motion commensurability. This resonance assures that Pluto is at aphelion when Pluto and Neptune are in conjunction, thus preventing close encounters. While resonances may stabilize the short-term evolution, they also give rise to the most prominent zones of instability.

The long-term stability of Pluto's orbit is thus of particular interest.

## NUMERICAL INTEGRATIONS WITH THE ORRERY

Historically, the long-term behavior of the solar system has been studied using perturbation theory. The interactions and the resulting motions are studied using series expansions that are expected to converge to the physically correct answers. In the secular theory (the first step in all such investigations), only those terms representing averages that are independent of the longitudes of the planets are considered (Brouwer and van Woerkom 1950; Brouwer and Clemence 1961). This may be thought of as treating the planets as massive rotating rings instead of point masses orbiting the Sun. Secular theory gives considerable insight into the long-term evolution of the planets, but it is only approximate and rapidly becomes intractable as it is extended to higher orders (see Anolik *et al.* 1969; Bretagnon 1974; Duriez 1979).

The development of computers made direct integrations of the equations of motion of the solar system possible. The first long-term integrations were made by Cohen and Hubbard (1965), who integrated the outer five planets for 120 000 yr, and Cohen, Hubbard, and Oesterwinter (1973, hereafter referred to as CHO), who extended the duration of the integration to 1 Myr. The time span covered by these integrations, though short compared to the age of the solar system, was long enough to reveal the previously unknown resonant stabilization mechanism for the orbit of Pluto described above (Cohen and Hubbard 1965; Brouwer 1966),

and to demonstrate (CHO) that the Brouwer and van Woerkom (1950) linear secular theory was a good approximation to many features of the motion of the outer five planets. Recently, the time interval over which the integration has been performed was extended to 5 Myr by Kinoshita and Nakai (1984).

Though direct, long-term numerical integrations have proven themselves to be powerful tools in celestial mechanics, their usefulness is limited by the availability of computer resources. If performed on a DEC VAX 11/780, one of the 100 Myr integration runs that we report here would require roughly one year. The reason for the large computing requirement is simple. The solar system is  $10^8$ – $10^{10}$  orbits old, depending on which orbit period is chosen for a reference, and the time step in a direct integration must be a small fraction of the orbit period. The computing time may be reduced to some extent by integrating equations of motion with the highest frequency variations removed by averaging (e.g., Schubart 1964; Williams and Benson 1971; Wisdom 1982). The averaging method has been quite useful for qualitative investigations. Unfortunately, the exact relationship between the averaged and unaveraged solutions is never clear. We integrate Newton's equations of motion for the solar system, modeling the bodies as point masses, as they stand. We have solved the computer-power problem by designing and building our own special-purpose computer, the Digital Orrery.

The Digital Orrery is a specialized but programmable high-performance computer designed for the efficient numerical integration of the equations of motion for systems with a small number of bodies that move in roughly circular orbits, e.g., the solar system. Details of the design and construction of the Orrery are discussed in Applegate *et al.* (1985). In an  $N$ -body system, the interaction of a body with the  $N - 1$  other bodies determines the force that will act on the body in each time step. In a serial computer, the computation of the forces requires  $O(N^2)$  time, while the integration step for  $N$  bodies requires  $O(N)$  time. The Orrery is a parallel computer with  $N$  concurrent processing units (planet computers) arranged in a ring. One processor is allocated for each body in the simplest programs. At each step, every processor executes identical instructions on different data. This arrangement allows the force computation to be accomplished in  $O(N)$  time and the integration step to be performed in  $O(1)$  time. Additionally, the Orrery  $N$ -body program is much more efficient than an  $N$ -body program written for a conventional computer. There are two reasons for this: The Orrery  $N$ -body program and the Orrery itself were designed together, with the result that there are essentially no wasted machine cycles; and the planet computers have a considerable amount of pipeline parallelism. Thus, though a planet computer does an isolated 64-bit floating point add or multiply in  $1.25 \mu\text{s}$  (roughly as fast as a VAX 11/780 with a floating-point accelerator) the Orrery can run a 10-body integration roughly 60 times faster than a VAX 11/780 with a floating-point accelerator.

#### OUR INTEGRATIONS

We used the Orrery to perform several integrations of the outer planets approximately 110 Myr forward in time and one integration approximately 107 Myr backward in time. We used the CHO initial conditions and masses, with the exception that we ran several Plutos as zero-mass test particles with various initial conditions. Whenever we refer to

“Pluto” we mean that particular test particle with the CHO initial conditions for Pluto. The main analysis reported in this paper was performed on a composite of a forward 106 776 073.9 yr run with a reverse 106 776 073.9 yr run for a total of 213 552 147.8 yr, or roughly 214 Myr.

We also did one run using the CHO mass of Pluto ( $M_{\text{Sun}}/(3.6 \times 10^5)$ ). This mass is far too large, but this run allowed us to compare our results for the first  $10^6$  yr with CHO. Over 110 Myr, the results of this run do not differ greatly from the results of the test-particle runs.

We employ the twelfth-order Stormer predictor used by CHO with time steps near 40 days in our outer-planet integrations. Since the truncation error of our predictor is smaller than the roundoff error due to the finite word length of the machine, no corrector is used. The Orrery has a 55-bit single-precision mantissa (it has 64-bit single-precision floating point). The performance of the integrator was improved by using double precision in certain crucial operations (Applegate *et al.* 1985). Stormer's predictor is a linear multistep integrator for second-order systems:

$$x_{n+1} = 2x_n \ominus x_{n-1} \oplus h^2(c_0 a_n + c_1 a_{n-1} + \dots + c_m a_{n-m}).$$

The circled operations are those where we used more than 64-bit precision.

The integrations are started using a combination of a fourth-order Runge-Kutta and the Stormer integrator. The Runge-Kutta is used to produce a starting set of accelerations and positions for the Stormer predictor. We start with a time step chosen to be less than a given value (we used 0.05 days) and such that the final time step is a power of two times the initial time step. The predictor is then used to advance the evolution until enough points are generated so that the Stormer predictor can be used again with double the step size. The step size is repeatedly doubled by this process until the desired step size is achieved.

The numerical error in our calculation caused a linear increase in the total energy of the system, as found by CHO, in contradiction to the prediction of Brouwer (1937) that the error in energy should grow as the square root of the number of steps. The linear energy error entails a quadratic longitude error because of the energy dependence of the mean motion. The fractional energy error after 110 Myr is  $2 \times 10^{-8}$ . This corresponds to a fractional energy error per year of  $1.8 \times 10^{-16}$ . The fractional energy error per year in CHO was  $2.4 \times 10^{-16}$ . By comparison, the relative mass lost by the Sun in 110 Myr due to electromagnetic radiation alone is about  $7.4 \times 10^{-6}$  (the mass lost due to solar wind is smaller by a factor of 4). Our energy error, which is almost entirely due to Jupiter, corresponds to an accumulated error in Jupiter's longitude of roughly  $100^\circ$  in 100 Myr. This error will not affect the secular variations of the orbits; it is only significant for phenomena that depend upon the relative longitudes of the planets, such as mean-motion resonances. The solar system has a number of approximate commensurabilities, but none are sufficiently exact for this integration error to change the low-order resonant structure of the system. The only exact commensurability is the Neptune-Pluto mean-motion resonance, but this resonance does not depend upon the longitude of Jupiter—the averaged integration of Williams and Benson (1971) shows it quite accurately. Thus the physical significance of much more accurate integrations is questionable.

In the Appendix, we give the initial values of the system state (center-of-mass coordinates and velocities) we used for

one typical 110 Myr integration and values of the system state that we obtained at 11 Myr intervals for the entire integration run. This should allow independent analysis of our integration error. This run was done with a 40 day step size using CHO masses, except that Pluto was given zero mass.

#### DATA AND INTERPRETATION

Each run evolved the system for a total simulated time of about 110 Myr (about  $10^9$  time steps with time steps near 40 days). Such a run takes roughly one week of real time. The positions and velocities of the planets and the Sun were read out once every  $10^5$  time steps, giving us a sampling period near 10 000 yr. The positions and velocities were converted to orbital elements, and the elements used to form the variables  $h$ ,  $k$ ,  $p$ , and  $q$  defined as

$$h = e \sin(\Omega + \omega); k = e \cos(\Omega + \omega),$$

$$p = \sin(i/2) \sin(\Omega); q = \sin(i/2) \cos(\Omega),$$

where  $i$  is the inclination,  $e$  is the eccentricity,  $\Omega$  is the longitude of the ascending node, and  $\omega$  is the argument of the perihelion. Thus  $\pi = \Omega + \omega$  is the longitude of perihelion. The linear secular theory is particularly simple when written in terms of the variables  $h$ ,  $k$ ,  $p$ , and  $q$ . The variables  $p$  and  $q$  specify the orientation of the orbital plane, and the variables  $h$  and  $k$  specify the eccentricity and the orientation of the orbit in the orbital plane.

Data in the time domain are difficult to digest, so most of the analysis was done in the frequency domain. High-resolution power spectra were obtained with the chirp  $z$ -transform algorithm (Rabiner, Schafer, and Rader 1969). Spectra

were examined using Hanning windows to suppress spectral leakage. We also made some low-resolution spectra with the ordinary fast Fourier transform (FFT) algorithm.

Our data are sampled at rather long periods (about 10 000 yr between samples) because of limited computer power available for analysis of the results (even at this rate a 110 Myr run yields about 5 Mbytes of ephemeris!). Consequently, the spectra we obtain are not band limited, so many of the lines are aliased versions of lines with periods shorter than 20 000 yr. Fortunately, aliased lines can be identified because their frequencies change if the sampling rate is changed. Real lines are stable under such a change of sampling rate. Thus we used the results of several runs with slightly different sampling periods to pick out the unaliased lines. These are then presented as tables of frequencies and amplitudes. Raw spectra of Jupiter's  $h$  and  $p$  are shown in Figs. 1 and 2, respectively. These figures show the full range from zero frequency to the Nyquist frequency,  $1.25 \times 10^{-7}$  cycles/day (about 1/20 000 yr). The dominant line in Jupiter's  $h$  corresponds to a period of 305 505 yr, and the large line in the center of the plot corresponds to a period of 45 906 years.

The frequencies and periods of the lines identified as the linear  $h - k$  and  $p - q$  features are listed in Table I along with the Brouwer and van Woerkom (1950) and Bretagnon (1974) predictions for the frequencies of these modes. In linear secular theory the interactions between the planets are averaged over mean longitudes, and only the lowest nonvanishing terms in eccentricity and inclination are kept. At this level of approximation, the equations of motion are linear and  $h$  and  $k$  are decoupled from  $p$  and  $q$ , yielding two normal

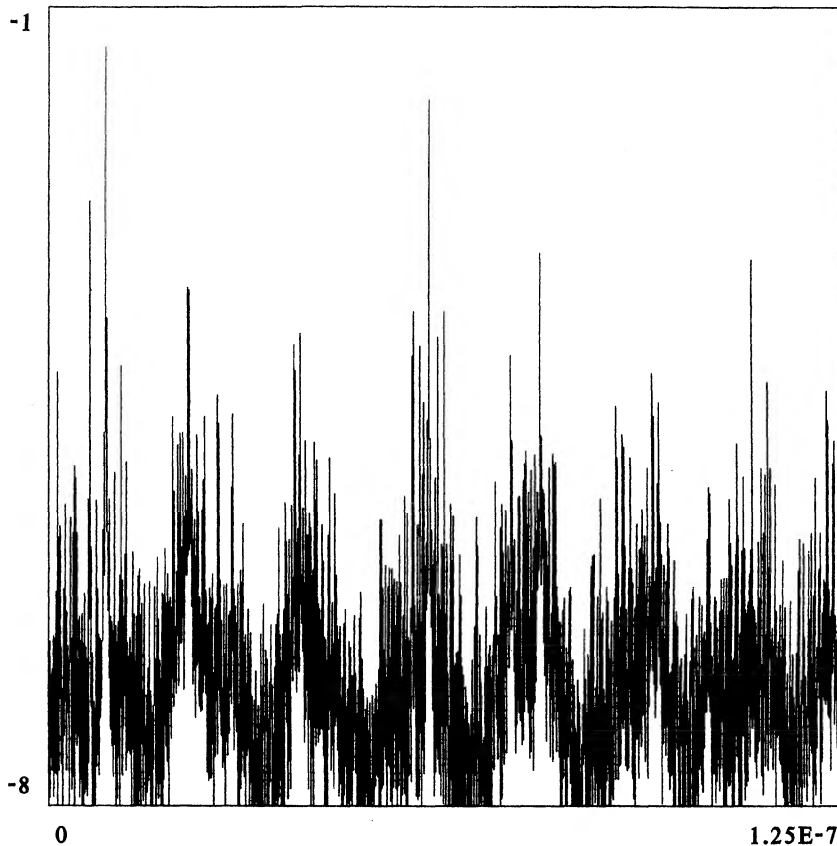


FIG. 1. Raw spectrum of Jupiter's  $h$ . The common logarithm of the amplitude is plotted against frequency (in cycles per day). The full range of frequencies, from 0 to  $1.25 \times 10^{-7}$  day $^{-1}$ , is shown. The large line in the center of the plot is the  $f_6$  line. The largest line on the left is the  $f_5$  line.

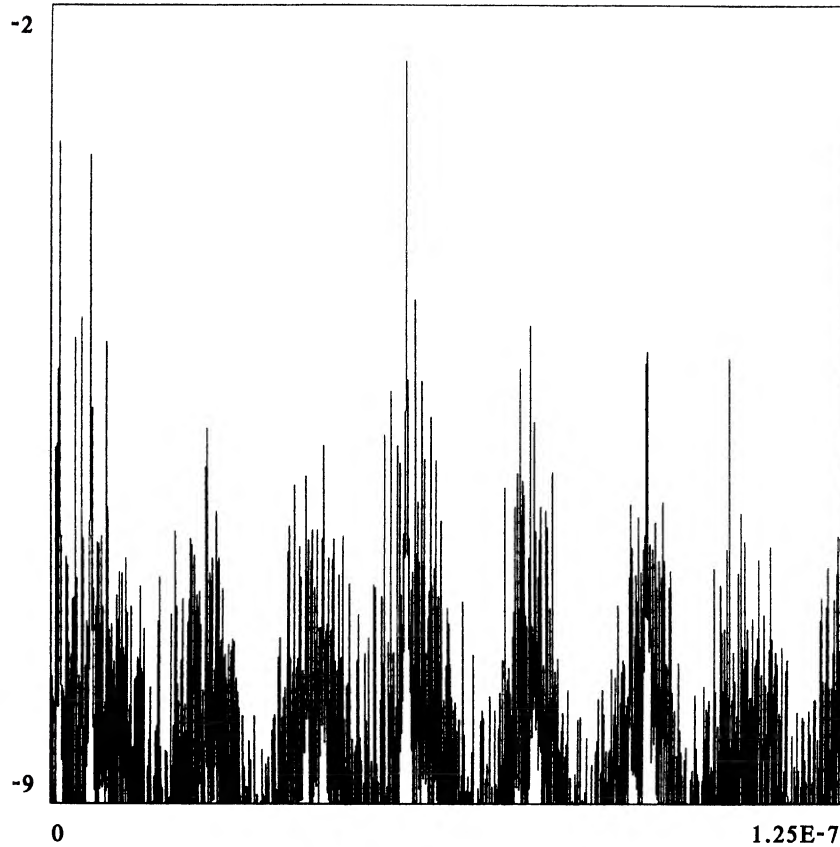


FIG. 2. Raw spectrum of Jupiter's  $p$ . The common logarithm of the amplitude is plotted against frequency. The full range of frequencies, from 0 to  $1.25 \times 10^{-7} \text{ day}^{-1}$ , is shown. The large line in the center of the plot is the  $g_6$  line.

modes of the system for each planet in the system. The motion of each planet is composed of a combination of the normal modes.

The conservation of angular momentum constrains the  $p - q$  equations so that one mode has zero frequency. Thus, for four planets there are four independent normal modes for the  $h - k$  spectra, and three independent normal modes for the  $p - q$  spectra. The  $p - q$  frequencies are denoted  $g_6, g_7,$  and  $g_8$ ; the  $h - k$  frequencies are denoted  $f_5, f_6, f_7,$  and  $f_8$ .  $g_5$  is the zero  $p - q$  frequency. The full  $N$ -body system has  $3N - 3$  independent frequencies, one for each degree of freedom. Thus the four planet (five-body) system has 12 independent frequencies. Four of these are the mean motions, leaving the eight secular frequencies, one of which is zero.

Nonlinearities in the secular theory produce linear combinations of the fundamental frequencies. The terms of the secular disturbing function are all even in the inclinations and in the eccentricities. For each term, the sum of the coefficients of the longitudes of perihelion and of the longitudes of ascending nodes must be zero so that the term is independent of the choice of reference direction. The sum of the coefficients of the longitudes of ascending nodes must be even so that the term is invariant under inversion of the reference plane. As a consequence, the sum of the coefficients of the longitudes of perihelia is also even. The amplitude of each term in the disturbing function is proportional to powers of the eccentricities, the inclinations, and the masses of the planets involved. In each term the difference of the power of

TABLE I(a). Fundamental frequencies as measured, compared with the theoretical predictions of Brouwer and van Woerkom and of Bretagnon. The measured frequencies are averages over the occurrences of the lines in the chirp  $z$ -transform spectra of each of the planets. Numbers in parentheses indicate the formal error (standard deviation) in the last digit shown.

	Measured		Br-vW	Bretagnon
	Period	Frequency	Frequency	Frequency
	yr	cycles/day	cycles/day	cycles/day
f8	1.924950e6	1.4222969e-9 (41)	1.33790e-9	1.410887e-9
f7	4.193511e5	6.5287787e-9 (51)	5.74464e-9	6.475315e-9
f6	4.590574e4	5.9640698e-8 (11)	5.86738e-8	5.538393e-8
f5	3.055056e5	8.9617245e-9 (1)	9.07527e-9	8.887885e-9
g8	1.872103e6	-1.4624465e-9 (16)	-1.43129e-9	-1.460675e-9
g7	4.327497e5	-6.3266380e-9 (1)	-6.13199e-9	-6.337273e-9
g6	4.921700e4	-5.5628146e-8 (1)	-5.43631e-8	-5.549021e-8
g5	---	---	---	---

TABLE I(b). Phases of fundamental lines as measured, compared with the theoretical predictions of Brouwer and van Woerkom and of Bretagnon. The measured phases are averages over the occurrences of the lines in the chirp  $z$ -transform spectra of each of the planets. Numbers in parentheses indicate the formal error (standard deviation) in the last digit shown.

	Measured		Br-vW	Bretagnon
	Radians	Degrees	Degrees	Degrees
f8	1.2870 (16)	73.742	69.431	72.090
f7	2.0769 (5)	118.997	131.944	114.775
f6	2.2193 (12)	127.155	131.686	127.715
f5	0.5242 (2)	30.032	31.174	28.503
g8	3.5521 (12)	203.518	202.293	201.288
g7	5.5886 (1)	320.202	315.063	316.293
g6	2.2228 (4)	127.359	127.366	125.643
g5	---	---	---	---

the inclination of each of the planets and the absolute value of the coefficient of the longitude of the corresponding node is even. Similarly, the difference of the power of the eccentricity and the absolute value of the corresponding coefficient of the longitude of perihelion is even. Since for secular terms the sum of the coefficients of the longitudes of ascending node must be even, the sum of the powers of the inclinations must also be even; and likewise for the eccentricities, the sum of the powers of the eccentricities must be even.

Short-period terms, those which depend on the mean longitudes, may also contribute to the long-period variations. In classical canonical perturbation theory, these terms may be removed at any particular order of the masses by a von Zeipel transformation. The new canonical variables differ from the old variables by a quantity of one higher order in the masses than the term eliminated from the disturbing function but divided by the frequency of the argument of the term. The new secular Hamiltonian is obtained as an average of the Hamiltonian expressed in terms of these new variables over the mean longitudes. A term can only have a nonzero average if it is multiplied by a term with the same frequency. Consequently, the sum of the powers of the eccentricities and the sum of the powers of the inclinations of any new term in the secular Hamiltonian are both even. Thus secular terms which arise in this way satisfy the same constraints as the original terms in the secular Hamiltonian. Since such terms contain factors of the frequency in the denominator, they only have a significant contribution if the frequency is small, i.e., near resonant. For example, the Hill corrections included by Brouwer and van Woerkom are of this type.

When written in terms of the variables  $h$ ,  $k$ ,  $p$ , and  $q$ , the sum of the powers of  $h$  and  $k$  is even, and the sum of the powers of  $p$  and  $q$  is even. The equations of motion for  $h$ ,  $k$ ,  $p$  and  $q$  contain derivatives of the disturbing function with respect to these variables. Thus the terms in the solutions for  $h$ ,  $k$ ,  $p$ , and  $q$  must be made up of odd numbers of fundamental frequencies. Indeed, terms in  $h$  and  $k$  must have an odd number of  $f$  frequencies and an even number of  $g$  frequencies; terms in  $p$  or  $q$  must have an even number of  $f$  frequencies and an odd number of  $g$  frequencies. Thus there should be no lines shared between the  $h - k$  and  $p - q$  solutions. Terms that produce combinations of three basic frequencies are two powers of small quantities smaller than the linear terms. Since the eccentricities, inclinations, and masses are all small, linear combinations of small numbers of the basic frequencies should dominate.

Table II lists major lines in the  $h - k$  and  $p - q$  spectra of the Jovian planets along with a proposed identification in terms of the fundamental frequencies identified with the frequencies predicted by the linear secular theory. Each entry in Table II(a) represents a contribution to  $h$  and  $k$ :

$$h = \sum_i \alpha_i \sin(2\pi r_i t + \delta_i),$$

$$k = \sum_i \alpha_i \cos(2\pi r_i t + \delta_i),$$

each entry in Table II(b) represents a contribution to  $p$  and  $q$ :

$$p = \sum_i \beta_i \sin(2\pi s_i t + \epsilon_i),$$

$$q = \sum_i \beta_i \cos(2\pi s_i t + \epsilon_i).$$

The amplitudes  $\alpha_i$  and  $\beta_i$  for each planet are represented by their common logarithms; the frequencies  $s_i$  and  $r_i$  are in inverse days.

These tables were produced by the following process. We started with the rectangular coordinate data, sampled at about 10 000 yr intervals, for a 214 Myr composite run. The 20 000 samples were converted to orbital elements and then to  $h$ ,  $k$ ,  $p$ , and  $q$  for each planet. (In Table III we provide a summary of the minimum, mean, and maximum values of the semimajor axes, the eccentricities, and the inclinations of the outer planets for a 214 Myr run.) We used a chirp  $z$  transform to make high-resolution spectra with 200 000 frequency-domain samples covering the full range of frequencies from zero to the Nyquist frequency. Possible lines were identified by finding all points in the spectrum higher than their nearest neighbors. The logarithms of the amplitudes at the peak were then fit with a parabola to determine the center frequency and amplitude of each potential line. The phases of each of the potential lines were determined by fitting a straight line to the phases of the same points. A typical  $h$  or  $k$  spectrum has about 1000 possible lines of logarithmic amplitude larger than  $-6.5$ . A typical  $p$  or  $q$  spectrum has about 200 possible lines of logarithmic amplitude larger than  $-6.5$ .

For each planet, the  $h$  and  $k$  line tables were compared. Potential lines were matched if the frequencies were within  $5.0 \times 10^{-12} \text{ day}^{-1}$  and if their amplitudes matched to within 0.1. If such a match was found, the line was accepted with the average of the matching frequency and amplitudes. The phases of both the  $h$  and  $k$  were preserved. Similar processing was done to merge the  $p$  and  $q$  spectra. Most lines passed this test. No potential lines were lost in  $h - k$  spectra with logarithmic amplitude greater than  $-5$  or in the  $p - q$  spectra with logarithmic amplitude greater than  $-5.5$ .

To remove aliases, the 214 Myr line tables were compared with line tables from two 110 Myr runs with different sampling rates. The 214 Myr composite run was sampled at intervals of 3 999 996 days. One 110 Myr comparison run (call it TP1) was sampled at intervals of 4 000 000 days, and the other 110 Myr comparison run (call it TP2) was sampled at intervals of 3 873 324 days. The TP1 comparison line table was produced using the same chirp  $z$  transform as was used in the 214 Myr run. The TP2 comparison line table was produced using an 8192-point Fourier transform. A line was considered real (unaliased) if it appeared in all three line tables, with a logarithmic amplitude tolerance of 0.1 and with a frequency tolerance of  $5.0 \times 10^{-12} \text{ day}^{-1}$  in the TP1 table and  $1.0 \times 10^{-11} \text{ day}^{-1}$  in the TP2 table. This reduced the number of distinct frequencies to 103.

Even with high-resolution spectra, the measurement of phase is numerically difficult. By contrast, the consistent measurement of frequencies and amplitudes was much easier; frequencies often matched predicted values to five significant places. For each distinct unaliased  $h - k$  line, we compared the  $h$  phase with the  $k$  phase (similarly for  $p - q$ ) to determine the sign of the frequency (because these should lead or lag by  $\pi/2$ ). In a few cases, the phases were inconsistent or ill defined. In these cases we were unable to give a good phase estimate or be sure of the sign of the frequency. No line of logarithmic amplitude larger than  $-5$  had a poorly defined phase. In Table II we mark occurrences of lines where there was substantial error in measurement of phase.

We then associated lines of the same frequency that oc-

TABLE II(a). Dominant  $h - k$  spectral lines for the Jovian planets in order of increasing frequency. Amplitudes are represented by their common logarithms. Frequencies and phases are averages of measured components in chirp  $z$  transforms. Phases are computed for J. D. 2430000.5. Components marked ( + ) have the given phase; components marked ( - ) have phase shifted by  $\pi$  from the given phase.

Identity	Period years	Frequency 1/days	Phase radians	Jupiter	Saturn	Uranus	Neptune
-f5+f7+f8	2.709005e+6	-1.010648e-9	2.8378	---	---	---	-4.25 (+)
+f8	1.924950e+6	1.422297e-9	1.2870	-4.23 (+)	-4.23 (+)	-2.77 (+)	-2.04 (+)
+f7+g7-g8	1.644681e+6	1.664670e-9	4.1099	---	---	---	-3.81 (-)
+f8+g7-g8	7.954332e+5	-3.441962e-9	3.3854	---	---	---	-5.64 (-)
-f7+f8+f8	7.431357e+5	-3.684187e-9	0.4977	---	---	---	-5.43 (+)
+f5-f7+f8	7.101583e+5	3.855268e-9	6.0136	-5.60 (-)	---	-4.30 (-)	-4.31 (-)
-f5+f7+f7	6.684161e+5	4.096027e-9	3.5053	-5.00 (+)	---	---	---
	6.682435e+5	4.097086e-9	1.7286	---	---	---	-4.84 (+)
	6.681535e+5	4.097636e-9	3.4529	---	---	-3.19 (+)	---
+f6+g6-g8	5.000501e+5	5.475153e-9	0.9037	---	---	-4.75 (+)	---
-f5+f8+f8	4.475731e+5	-6.117103e-9	2.0439	---	---	---	-5.58 (-)
+f8-g7+g8	4.354766e+5	6.287022e-9	5.5236	-5.36 (+)	---	-4.12 (+)	---
+f7	4.193511e+5	6.528779e-9	2.0769	-2.73 (+)	-2.81 (+)	-1.54 (+)	-2.43 (-)
	3.609930e+5	7.584221e-9	2.1969	-5.36 (+)	---	---	---
	3.462663e+5	??.906777e-9	??	---	---	-5.47	---
+f5	3.055049e+5	8.961725e-9	0.5242	-1.35 (+)	-1.48 (+)	-1.42 (-)	-2.71 (+)
+f6+g6-g7	2.647994e+5	1.033934e-8	5.1811	-5.07 (+)	-4.96 (+)	-4.31 (-)	-5.55 (+)
+f5+f5-f7	2.402751e+5	1.139465e-8	5.2796	-4.16 (-)	-4.34 (-)	-3.34 (+)	-4.20 (-)
+f7+f7-f8	2.353096e+5	1.163510e-8	2.9233	---	---	-4.98 (-)	-5.13 (+)
+f5-g7+g8	1.980214e+5	1.382603e-8	4.6633	---	---	---	-5.26 (+)
	1.980122e+5	1.382668e-8	1.2765	---	---	-5.10 (+)	---
+f5+f7-f8	1.946128e+5	1.406820e-8	1.3116	---	---	-4.89 (+)	-4.86 (-)
-f7+g7+g8	1.912215e+5	-1.431769e-8	0.7791	---	---	-5.35 (+)	-5.64 (-)
+f5+f5-f8	1.659193e+5	1.650110e-8	6.0467	-6.08 (-)	---	---	-5.15 (+)
-f5+g7+g8	1.634486e+5	-1.675053e-8	2.2897	---	---	-5.35 (-)	-5.57 (+)
-f7+g7+g7	1.427337e+5	-1.918153e-8	2.7827	---	---	-5.39 (-)	-5.80 (+)
	1.266758e+5	??.161305e-8	??	---	---	-5.07	---
+f5+g6-g7	6.787014e+4	-4.033955e-8	3.4610	---	---	-5.22 (+)	---
+f5+f5-f6	6.562875e+4	-4.171725e-8	5.1131	-4.86 (+)	-3.85 (-)	-4.37 (+)	---
+f5-f6+f7	6.201225e+4	-4.415016e-8	0.3790	-5.48 (+)	-4.74 (-)	-4.42 (-)	---
-f5+f6+f8	5.254864e+4	5.210127e-8	2.9811	-5.46 (+)	-4.98 (-)	---	---
+f6-f7+f8	5.020428e+4	5.453421e-8	1.4081	-6.08 (+)	---	---	---
+f7-g6+g7	4.903883e+4	5.583026e-8	5.4446	-5.32 (+)	-4.84 (-)	---	---
	4.875614e+4	5.615397e-8	2.5887	-5.48 (+)	---	---	---
B -f5+f6+f7	4.785814e+4	5.720763e-8	3.7831	-3.70 (+)	-3.23 (-)	---	---
D +f5-g6+g7	4.699110e+4	5.826317e-8	3.8835	-3.98 (-)	-3.50 (+)	-4.74 (-)	---
F	4.673179e+4	5.858647e-8	1.3458	-5.07 (-)	-4.59 (+)	---	---
A +f6	4.590575e+4	5.964070e-8	2.2193	-1.80 (-)	-1.32 (+)	-2.81 (-)	-3.99 (-)
G +f7-g6+g8	4.510871e+4	6.069451e-8	3.3787	-5.13 (+)	---	---	---
E	4.486943e+4	6.101818e-8	0.5474	-3.93 (+)	-3.44 (-)	---	---
C +f5+f6-f7	4.410649e+4	6.207365e-8	0.6658	-3.71 (-)	-3.21 (+)	---	---
+f5-g6+g8	4.337023e+4	6.312742e-8	1.8581	-5.40 (-)	-4.90 (+)	---	---
	4.314901e+4	6.345107e-8	2.1368	-5.47 (+)	-4.98 (-)	---	---
	4.244300e+4	6.450653e-8	2.1315	-5.77 (+)	-5.28 (-)	---	---
+f6+f7-f8	4.228564e+4	6.474659e-8	2.9744	---	-5.66 (+)	---	---
+f5+f6-f8	4.075388e+4	6.718013e-8	1.4533	-5.48 (-)	-4.99 (+)	---	---
	3.860593e+4	-7.091788e-8	3.5400	---	---	-5.70 (+)	---
	2.570531e+4	1.065091e-7	4.0056	---	-5.84 (+)	---	---
	2.537709e+4	1.078867e-7	5.4694	-4.82 (+)	-4.29 (-)	---	---
+f6-g6+g7	2.513122e+4	1.089422e-7	5.5879	-5.14 (-)	-4.60 (+)	---	---
	2.482061e+4	??.103055e-7	??	---	---	-4.86 (+)	---
-f5+f6+f6	2.481743e+4	1.103197e-7	3.9121	-3.24 (-)	-2.72 (+)	-4.38 (-)	-5.61 (-)
	2.451136e+4	1.116972e-7	2.2469	-5.07 (+)	-4.54 (-)	---	---
+f6+f6-f7	2.428192e+4	1.127527e-7	2.3600	-4.30 (-)	-3.77 (+)	---	---
+f6+f6-f8	2.322986e+4	1.178591e-7	3.1472	-5.71 (-)	---	---	---

Phase measurement errors:

- ? in sign of frequency: sign of frequency undetermined - bad phase
- ? after phase: best phase estimate assuming positive frequency
- ?? in place of phase: phase errors too large to determine phase

TABLE II(b). Dominant  $p - q$  spectral lines for the Jovian planets in order of increasing frequency. Amplitudes are represented by their common logarithms. Frequencies and phases are averages of measured components in chirp  $z$  transforms. Phases are computed for J. D. 2430000.5. Components marked ( + ) have the given phase; components marked ( - ) have phase shifted by  $\pi$  from the given phase.

Identity	Period years	Frequency 1/days	Phase radians	Jupiter	Saturn	Uranus	Neptune
+f5-f7+g8	2.821078e+6	9.704982-10	2.0022	-5.84 (-)	-5.82 (-)	-5.41 (-)	-4.75 (+)
+f7-f8+g7	2.244532e+6	-1.219787e-9	0.1404	-5.26 (+)	-5.27 (+)	-5.61 (-)	-4.24 (-)
+g8	1.872103e+6	-1.462447e-9	3.5521	-3.24 (-)	-3.25 (-)	-3.25 (+)	-2.24 (+)
+f6-f7+g6	1.088082e+6	-2.516218e-9	2.3641	---	---	-4.58 (-)	-4.78 (+)
+f7-f8+g8	7.513253e+5	3.644029e-9	4.3527	---	---	---	-5.82 (+)
+f5-f7+g7	7.031687e+5	-3.893590e-9	3.8723	-4.96 (-)	-5.00 (-)	-3.74 (+)	---
	7.029241e+5	-3.894945e-9	1.6392	---	---	---	-4.70 (+)
	6.619870e+5	-4.135808e-9	1.1958	---	---	-5.85 (+)	---
T -f5+f6+g6	5.531944e+5	-4.949165e-9	3.9167	-4.76 (-)	-5.23 (+)	-3.53 (+)	-4.25 (-)
	4.555939e+5	-6.009411e-9	2.9019	---	---	-6.15 (+)	---
+f5-f8+g8	4.505195e+5	76.077098e-9	2.7833?	---	---	---	-6.01 (-)
+g7	4.327497e+5	-6.326638e-9	5.5886	-3.32 (-)	-3.41 (-)	-2.05 (+)	-2.97 (-)
-f7+f8+g8	4.168010e+5	-6.568724e-9	2.7633	-5.51 (-)	-5.61 (-)	-4.23 (+)	-5.07 (-)
	3.708698e+5	-7.382243e-9	2.3494	---	---	-5.48 (+)	-6.03 (-)
-f5+f7+g7	3.125550e+5	-8.759581e-9	0.8577	-5.00 (+)	-5.15 (+)	-3.71 (-)	-4.55 (+)
-f5+f8+g8	3.041431e+5	-9.001850e-9	4.3144	---	---	-5.10 (-)	-5.73 (+)
	2.446399e+5	-1.119135e-8	4.8619	---	---	---	-6.02 (+)
	2.446353e+5	-1.119156e-8	2.0267	---	---	-5.50 (+)	---
-f7+f8+g7	2.394675e+5	-1.143308e-8	4.7639	---	---	-5.58 (-)	-5.76 (+)
+f5+f8-g8	2.311113e+5	1.184646e-8	4.5730	---	---	-6.15 (-)	---
-f5+f8+g7	1.974497e+5	-1.386607e-8	0.0675	---	---	-5.93 (+)	-5.78 (-)
+f7+f8-g7	1.917571e+5	1.427770e-8	4.0751	---	---	-6.15 (-)	-6.16 (+)
+f7+f7-g8	1.885576e+5	1.451997e-8	0.5989	---	---	-5.76 (-)	-5.80 (+)
+f5+f8-g7	1.638385e+5	1.671067e-8	2.5067	---	---	---	-6.11 (-)
+f5+f7-g8	1.614973e+5	1.695292e-8	5.3655	---	---	-5.45 (+)	-5.46 (-)
+f7+f7-g7	1.412412e+5	1.938423e-8	4.9353	---	---	-5.52 (+)	---
-f5-f6+g8	1.412312e+5	-1.938559e-8	2.5706	---	---	---	-5.55 (+)
+f5+f7-g7	1.254908e+5	2.181715e-8	3.3018	---	---	-4.91 (-)	-5.28 (+)
	1.196968e+5	2.287322e-8	3.4271	---	---	-6.16 (+)	---
+f5+f5-g7	1.129007e+5	2.425008e-8	1.7432	-6.08 (-)	-5.94 (-)	-4.71 (+)	-5.51 (-)
	1.026066e+5	2.668298e-8	3.3569	---	---	-6.12 (+)	---
-f5+f6+g7	6.172963e+4	4.435229e-8	1.0016	---	-5.89 (+)	-5.12 (-)	---
	5.987014e+4	4.572982e-8	5.6122	---	-6.09 (+)	---	---
+f6-f7+g7	5.851960e+4	4.678520e-8	5.7446	---	---	-5.62 (+)	---
-f5+f6+g8	5.562908e+4	4.921618e-8	5.3260	---	---	-6.13 (-)	---
+f5-f6+g8	5.250838e+4	-5.214121e-8	1.8790	-5.81 (-)	-5.43 (+)	-6.16 (+)	---
+f5-f7+g6	5.146803e+4	-5.319517e-8	0.6683	-5.42 (+)	-4.98 (-)	-5.33 (+)	---
	5.046667e+4	-5.425067e-8	3.6929	-5.86 (+)	-5.47 (-)	---	---
-f6+f7+g8	5.016749e+4	-5.457420e-8	3.2458	-6.00 (+)	-5.61 (-)	---	---
+g6	4.921701e+4	-5.562815e-8	2.2228	-2.50 (-)	-2.10 (+)	-3.45 (-)	-4.42 (-)
+f5-f6+g7	4.802774e+4	-5.700561e-8	3.8941	-4.63 (+)	-4.22 (-)	-4.98 (+)	---
-f5+f7+g6	4.715469e+4	-5.806104e-8	3.7830	-5.34 (-)	-4.98 (+)	-5.45 (+)	---
-f6+f7+g7	4.606187e+4	-5.943856e-8	5.4459	-5.62 (-)	-5.18 (+)	-5.49 (-)	---
+f5+f7-g6	3.849691e+4	7.111871e-8	0.3775	---	-5.99 (+)	-5.81 (+)	---
+f5+f5-g6	3.722354e+4	7.355159e-8	5.1076	-5.21 (-)	-4.80 (+)	-5.64 (-)	---
+f5+f6-g7	3.653929e+4	7.492896e-8	3.4386	---	-5.81 (-)	-5.17 (+)	---
+f5-f6+g6	2.575416e+4	-1.063071e-7	0.5274	-5.14 (+)	-5.10 (-)	-5.43 (-)	---
-f6+f7+g6	2.517795e+4	-1.087400e-7	2.0771	---	---	-5.88 (+)	---
+f5+f6-g6	2.203846e+4	1.242306e-7	0.5211	-5.07 (+)	-4.70 (-)	-5.33 (-)	---

Phase measurement errors:

? in sign of frequency: sign of frequency undetermined - bad phase

? after phase: best phase estimate assuming positive frequency

?? in place of phase: phase errors too large to determine phase

TABLE II(c). Given the frequencies and phases measured for the fundamental lines, we compute the frequencies and phases of the combination lines that occur in our data. Here we have predicted (not measured) frequencies and phases, and the differences between the measured and predicted values.

<i>h - k</i> lines					<i>p - q</i> lines				
Identity	Frequency	Error	Phase	Error	Identity	Frequency	Error	Phase	Error
-f5+f7+f8	-1.010649d-09	9.000d-16	2.8398	-0.0020	+f5-f7+g8	9.704993d-10	-1.100d-15	1.9993	0.0029
f8	1.422297d-09	1.000d-16	1.2870	-0.0000	+f7-f8+g7	-1.220156d-09	3.692d-13	0.0952	0.0452
+f7+g7-g8	1.664587d-09	8.280d-14	4.1134	-0.0035	+g8	-1.462447d-09	-5.000d-16	3.5521	0.0000
+f8+g7-g8	-3.441895d-09	-6.740d-14	3.3236	0.0618	+f6-f7+g6	-2.516227d-09	8.700d-15	2.3652	-0.0011
-f7+f8+f8	-3.684185d-09	-2.100d-15	0.4972	0.0005	+f7-f8+g8	3.644035d-09	-6.300d-15	4.3419	0.0108
+f5-f7+f8	3.855243d-09	2.530d-14	6.0175	-0.0039	+f5-f7+g7	-3.893692d-09	1.022d-13	4.0358	-0.1635
-f5+f7+f7	4.095833d-09	1.941d-13	3.6296	-0.1243	-f5+f6+g6	-4.949173d-09	7.500d-15	3.9180	-0.0013
+f6+g6-g8	5.474998d-09	1.545d-13	0.8901	0.0136	+f5-f8+g8	6.076981d-09	1.169d-13	2.7892	-0.0059
-f5+f8+f8	-6.117131d-09	2.770d-14	2.0499	-0.0060	+g7	-6.326638d-09	-1.034d-25	5.5886	0.0000
+f8-g7+g8	6.286488d-09	5.336d-13	5.5337	-0.0101	-f7+f8+g8	-6.568928d-09	2.043d-13	2.7622	0.0011
+f7	6.528779d-09	3.000d-16	2.0769	0.0000	-f5+f7+g7	-8.759584d-09	2.800d-15	0.8581	-0.0004
+f5	8.961725d-09	5.000d-16	0.5242	0.0000	-f5+f8+g8	-9.001874d-09	2.410d-14	4.3149	-0.0005
+f6+g6-g7	1.033919d-08	1.500d-13	5.1367	0.0444	-f7+f8+g7	-1.143312d-08	3.980d-14	4.7987	-0.0448
+f5+f5-f7	1.139467d-08	-2.030d-14	5.2546	0.0250	+f5+f8-g8	1.184647d-08	-7.900d-15	4.5423	0.0307
+f7+f7-f8	1.635262d-08	-1.605d-13	2.8667	0.0566	-f5+f8+g7	-1.386607d-08	-4.400d-15	0.6683	-0.0008
+f5-g7+g8	1.382592d-08	1.140d-13	4.7708	-0.1075	+f7+f8-g7	1.427771d-08	-1.360d-14	4.0585	0.0166
+f5+f7-f8	1.406821d-08	-6.300d-15	1.3140	-0.0024	+f7+f7-g8	1.452000d-08	-3.390d-14	0.6017	-0.0028
-f7+g7+g8	-1.431786d-08	1.732d-13	0.7806	-0.0015	+f5+f8-g7	1.671066d-08	1.060d-14	2.5058	0.0009
+f5+f5-f8	1.650115d-08	-5.210d-14	6.0445	0.0022	+f5+f7-g8	1.695295d-08	-2.970d-14	5.3322	0.0333
-f5+g7+g8	-1.675081d-08	2.790d-13	2.3333	-0.0436	+f7+f7-g7	1.938420d-08	3.460d-14	4.8484	0.0869
-f7+g7+g7	-1.918205d-08	5.247d-13	2.8171	-0.0344	-f5-f5+g8	-1.938590d-08	3.055d-13	2.5037	0.0669
+f5+g6-g7	-4.033978d-08	2.335d-13	3.4416	0.0194	+f5+f7-g7	2.181714d-08	8.800d-15	3.2957	0.0061
+f5+f5-f6	-4.171725d-08	-1.000d-15	5.1122	0.0009	+f5+f5-g7	2.425009d-08	-7.000d-15	1.7429	0.0003
+f5-f6+f7	-4.415019d-08	3.480d-14	0.3818	-0.0028	-f5+f6+g7	4.435234d-08	-4.550d-14	1.0005	0.0011
-f5+f6+f8	5.210127d-08	-4.000d-16	2.9822	-0.0011	+f6-f7+g7	4.678528d-08	-8.130d-14	5.7310	0.0136
+f6-f7+f8	5.453422d-08	-6.200d-15	1.4294	-0.0213	-f5+f6+g8	4.921653d-08	-3.470d-13	5.2472	0.0788
+f7-g6+g7	5.583029d-08	-2.670d-14	5.4426	0.0020	+f5-f6+g8	-5.214142d-08	2.100d-13	1.8569	0.0221
-f5+f6+f7	5.720775d-08	-1.222d-13	3.7720	0.0111	+f5-f7+g6	-5.319520d-08	3.020d-14	0.6701	-0.0018
+f5-g6+g7	5.826323d-08	-6.250d-14	3.8899	-0.0064	-f6+f7+g8	-5.457437d-08	1.658d-13	3.4097	-0.1639
+f6	5.964070d-08	2.000d-15	2.2193	0.0000	+g6	-5.562815d-08	-4.000d-15	2.2228	-0.0000
+f7-g6+g8	6.069448d-08	3.180d-14	3.4061	-0.0274	+f5-f6+g7	-5.700561d-08	1.500d-15	3.8934	0.0007
+f5+f6-f7	6.207364d-08	6.200d-15	0.6665	-0.0007	-f5+f7+g6	-5.806109d-08	5.180d-14	3.7756	0.0074
+f5-g6+g8	6.312742d-08	-4.000d-15	1.8534	0.0047	-f6+f7+g7	-5.943856d-08	-2.700d-15	5.4462	-0.0003
+f6+f7-f8	6.474718d-08	-5.898d-13	3.0091	-0.0347	+f5+f7-g6	7.111865d-08	6.080d-14	0.3782	-0.0007
+f5+f6-f8	6.718013d-08	4.400d-15	1.4564	-0.0031	+f5+f5-g6	7.355160d-08	-5.000d-15	5.1087	-0.0011
+f6-g6+g7	1.089422d-07	-6.000d-15	5.5850	0.0029	+f5+f6-g7	7.492906d-08	-1.005d-13	3.4380	0.0006
-f5+f6+f6	1.103197d-07	2.850d-14	3.9144	-0.0023	+f5-f6+g6	-1.063071d-07	1.950d-14	0.5277	-0.0003
+f6+f6-f7	1.127526d-07	8.270d-14	2.3617	-0.0017	-f6+f7+g6	-1.087401d-07	6.530d-14	2.0804	-0.0033
+f6+f6-f8	1.178591d-07	9.000d-16	3.1515	-0.0043	+f5+f6-g6	1.242306d-07	3.150d-14	0.5206	0.0005

curred in the corresponding spectra of more than one planet. An identification was made if the frequencies matched to within  $5.0 \times 10^{-12} \text{ day}^{-1}$ . We then checked the phases and the signs of the frequencies for consistency (phases had to be within 0.2 radians of each other, allowing a shift by  $\pi$ ). This caused the disambiguation of a few lines, and allowed us to determine the phases of a few lines for which either the *h* or the *k* phase had serious measurement error. Consistent sets were then given averaged frequencies and phases.

We hand selected the fundamental frequencies  $\{f_i, g_i\}$  to be the largest lines in the vicinity of the Brouwer and van Woerkom predictions. We then generated all possible additive combinations of up to three fundamental frequencies. We attempted to identify each line with one of these combinations according to frequency and phase. Just as the frequencies of a combination are formed by adding and subtracting frequencies of fundamental lines, the phases of a combination are formed by adding and subtracting the phases of fundamental lines. An identification was made if the frequencies matched to within  $5.0 \times 10^{-12} \text{ day}^{-1}$  and the

phases matched to within 0.2 radians. These allowed further disambiguation of a few lines and confirmed the classification. In identification of lines there are 287 distinct combinations with three or fewer fundamental frequencies. Of the 103 lines we find, 23 could not be assigned to a combination of three frequencies.

The amplitude coefficients may be either positive or negative. A negative amplitude may be viewed as a positive amplitude with the phase rotated by  $\pi$ . Since we are specifying the amplitudes with the logarithms of the absolute values, we also provide the sign. In Table II we indicate the sense of the match of the measured phase of a line with the phase implied by its identification label using the symbols “(+)” and “(-)”.

Even the comparison of only two runs eliminates most aliases. For the looser case (TP2), the spectra were effectively divided into about 240 000 bins. There are 12 000 bins in frequency and about 20 bins in amplitude ( $\Delta f \approx 1.0 \times 10^{-11} \text{ day}^{-1}$ ,  $f_{\text{max}} = 1.25 \times 10^{-7} \text{ day}^{-1}$ ). Thus the expected number of coincidences in a sample of 1000 randomly distributed

TABLE III. Variations of the semimajor axes  $a$ , the eccentricities  $e$ , and the inclinations  $i$  of the outer planets over 214 Myr.  $a$  is in AU,  $i$  is in radians,  $i$  is measured relative to the invariable plane of CHO.

	minimum	mean	maximum
<b>Jupiter</b>			
a:	5.20135E+000	5.20257E+000	5.20487E+000
e:	2.52206E-002	4.56015E-002	6.18055E-002
i:	2.83801E-003	6.45747E-003	9.76233E-003
<b>Saturn</b>			
a:	9.51297E+000	9.55488E+000	9.59206E+000
e:	8.01269E-003	5.36152E-002	8.90992E-002
i:	1.24408E-002	1.57810E-002	1.90587E-002
<b>Uranus</b>			
a:	1.91016E+001	1.92183E+001	1.93320E+001
e:	7.01759E-004	4.39952E-002	7.61826E-002
i:	1.40198E-002	1.78314E-002	2.15983E-002
<b>Neptune</b>			
a:	2.99143E+001	3.01098E+001	3.03168E+001
e:	7.58230E-005	1.01261E-002	2.28723E-002
i:	7.89724E-003	1.17275E-002	1.52102E-002
<b>Pluto</b>			
a:	3.89838E+001	3.94559E+001	3.99831E+001
e:	2.07307E-001	2.44315E-001	2.80581E-001
i:	2.55640E-001	2.78190E-001	2.97766E-001

frequencies is less than 4. The use of two different runs of two different sampling rates essentially guarantees that no aliases survive.

#### COMPARISON WITH THE SECULAR THEORY

To date, the most complete secular theory for the entire solar system is that of Bretagnon (1974). Except for the  $f_6$  frequency, Bretagnon's predictions agree with our measurements more closely than do Brouwer and van Woerkom's predictions. Bretagnon's  $f_6$  frequency appears to be in error by more than seven parts in 100. We assert with confidence that this difference is not a consequence of the fact that Bretagnon's theory is for eight planets and we only simulated the Jovian planets. To verify this fact, we made a 3 Myr run of the Jovian planets with Venus, Earth, and Mars. The  $f_6$  frequency as determined in the 3 Myr run differed from the  $f_6$  frequency as determined in our 110 Myr runs by only 1 part in  $10^4$ . The  $g_6$  frequency determinations differed by three parts in  $10^4$ .

Many of the lines we measure are identifiable with those predicted by Bretagnon. As expected, we observe no line that appears in both the  $h$  and  $p$  spectra of any planet. Each line is either an  $h$  line or a  $p$  line and it obeys the constraints on formation described above. The amplitudes of the fundamental frequencies are quite what is expected. We see none of the two-frequency combinations, such as  $f_5 + g_5 - g_7$  (remember that  $g_5 = 0$ ), predicted by Bretagnon. This is because our osculating elements are referenced to the invariable plane and Bretagnon uses ecliptic elements. We pick up those lines when we use ecliptic elements to represent the results of our integrations. Except for those lines, the spectra of  $h$  and  $p$  do not depend on the choice of the osculating-element reference plane.

However, there are some major discrepancies between our measured amplitudes and Bretagnon's amplitudes for combinations of the fundamental frequencies. For example, the lines marked  $F$  and  $E$  in Table II cannot be constructed as a

combination of three or fewer fundamental frequencies. These lines are not included by Bretagnon, since he only included terms up to third order in inclinations and eccentricities and second order in the masses. However, the amplitudes of these lines are considerably larger than the amplitudes of many of the terms included by Bretagnon. Line  $E$  in Saturn's  $h$  spectrum has an amplitude of  $3.63 \times 10^{-4}$  (with logarithm  $-3.44$ ). This is larger than all but seven of Bretagnon's more than 200 corrections to the Lagrange solution for the Jovian planets. Even for identified lines, there are serious differences. For example, line  $D$  is identified as  $f_5 - g_6 + g_7$  (in Bretagnon's notation  $\psi_5 - \theta_6 + \theta_7$ ). Bretagnon predicts the amplitude for Jupiter to be  $1.0 \times 10^{-6}$  and for Saturn to be  $6.0 \times 10^{-6}$ . We measure these to be  $1.0 \times 10^{-4}$  and  $3.2 \times 10^{-4}$ , respectively. The major discrepancies in  $h$  lines appear to be clustered around the  $4.59 \times 10^4$  yr  $f_6$  line that we noted before to be discrepant in frequency, but this is not the whole story. Line  $T$ , in the  $p$  spectrum of Uranus, is a low-frequency line (period about  $5.53 \times 10^5$  yr) that is predicted to be of amplitude  $4.6 \times 10^{-5}$ , but we measure it to be about  $3.0 \times 10^{-4}$ . We note a large number of discrepancies between the measured amplitudes and the amplitudes predicted by Bretagnon. Bretagnon also predicts a number of very small lines that we do not detect. It is possible that these small differences are a result of measurement errors introduced by nearby larger lines in the spectrum.

Some insight into the origin of these discrepancies can be derived by an examination of the fine structure of the spectrum near the  $f_6$  line. Figure 3 shows a high-resolution view of this region of the raw spectrum of Jupiter's  $h$ . The large central line, labeled  $A$ , is the  $f_6$  line. The  $f_6$  line is surrounded by a cluster of smaller lines. The lines marked "\*" are aliases of high-frequency undersampled components; they moved in runs with different sampling rates. We can see that the  $f_6$  line is bracketed by a symmetrical group of lines. The outermost members of the group, labeled  $B$  and  $C$ , are  $-f_5 + f_6 + f_7$  and  $f_5 + f_6 - f_7$ .  $D$  and  $E$ , and  $F$  and  $G$ , are also symmetrically placed around  $f_6$ . Evidently, the  $f_6$  line is modulated with three dominant modulating frequencies. The line labeled  $D$  is identified as  $f_5 - g_6 + g_7$ . The symmetrical line, labeled  $E$ , has no identification. However, because of the symmetry we can deduce that this line is actually  $-f_5 + 2f_6 + g_6 - g_7$ . Similarly, since  $G$  is identified as  $f_7 - g_6 + g_8$  we can deduce that  $F$  must be  $2f_6 - f_7 + g_6 - g_8$ . Thus the major contribution to the amplitudes of the  $D$  and  $G$  lines must be fifth-order combinations rather than third-order combinations. For example, we may identify  $D$  as  $f_6 - (-f_5 + f_6 + g_6 - g_7)$  and  $E$  as  $f_6 + (-f_5 + f_6 + g_6 - g_7)$ . The fifth-order labeling of  $E$  is confirmed by the agreement of the phase combination with the measured phase. The phase predicted by our labeling of the  $F$  line is not quite so accurately confirmed, but the  $F$  line is a very small line close to very large lines. The problem with Bretagnon's analysis is that higher-order terms that he did not include are more important than most of the terms he included. Duriez (1979) has constructed a theory (for only the outer planets) including seventh-order terms, and indeed his prediction of the  $f_6$  frequency is correct to 1 part in 300, but his  $f_5$  frequency is still in error by more than 1 part in 100.

#### THE ORBIT OF PLUTO

Pluto's orbit crosses that of Neptune and it is substantially inclined to the ecliptic. It is protected from a close encounter

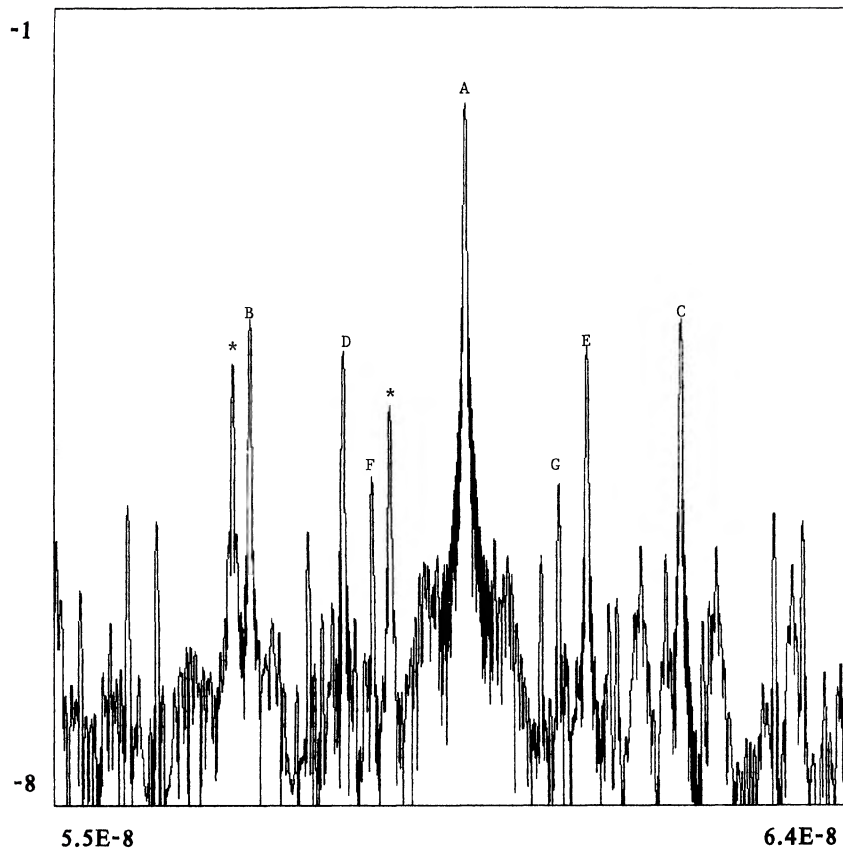


FIG. 3. Expanded view of Jupiter's  $h$  spectrum around the region of the  $f_6$  line. The common logarithm of the amplitude is plotted against frequency. The line marked  $A$  is the  $f_6$  line. Lines marked "\*" are aliases. Note the symmetrical sextuplet of lines surrounding  $f_6$ . The strong pair marked  $D$  and  $E$  is not taken into account in theories that only consider terms that are of third order in inclinations and eccentricities and second order in the masses.

with Neptune by the libration of the resonant argument  $3\lambda_{\text{Pluto}} - 2\lambda_{\text{Neptune}} - \pi_{\text{Pluto}}$ . This resonance has a period of about 19 857 yr; the resonant argument varies about  $\pi$  between  $-1.5$  and  $1.5$  radians ( $-86^\circ$  to  $86^\circ$ ). Williams and Benson (1971) demonstrated that Pluto also takes part in a complex resonance of the argument of perihelion ( $\omega$ ), with a period of about 3.796 Myr. Nacozy and Diehl (1978) developed a semianalytical theory of this libration. Figure 4 shows the evolution of the argument of perihelion over the full 214 Myr. The 3.796 Myr libration about  $\pi/2$  is amplitude modulated with a period near 34 Myr.

In the power spectrum of the resonant argument, there are numerous lines near that point in the spectrum where the 19 857 yr libration period should appear. (Since the libration period is undersampled, the group appears in an aliased position in the spectrum.) Figure 5 shows an expanded view of this region. What we see is a broad peak centered around a period of 19 857 yr consisting of numerous sharper peaks separated by a frequency corresponding to a period of 3.69 Myr. This spectrum is characteristic of narrowband frequency modulation. Evidently, the frequency of the mean-motion libration is modulated by the circulation of the longitude of the ascending node.

The variation of the argument of perihelion is locked to the variations of the eccentricity and the inclination (Williams and Benson 1971). This coupling is illustrated in Fig. 6, where the inclination is plotted versus the argument of perihelion. The 34 Myr variation appears as a slow expansion and contraction of the nearly circular trajectory on this  $i$  versus  $\omega$  plot. The 34 Myr period seen in the argument of perihelion is even more pronounced in the inclination. In

Fig. 7, we see that the 34 Myr modulation of the inclination has an additive as well as a multiplicative component. In addition, there seems to be a much longer period present. This longer period is due to a near commensurability between  $g_8$  and the period of circulation of the ascending node.

Because of the libration of the argument of perihelion, the  $h - k$  and  $p - q$  degrees of freedom are more intimately coupled for Pluto than they are for the other planets. The  $h - k$  and  $p - q$  spectra of the Jovian planets have no lines in common; Pluto's  $h - k$  and  $p - q$  spectra have many lines in common. Now we expect the  $h - k$  and  $p - q$  spectra of Pluto to contain combinations of two new fundamental frequencies (which correspond to the two long-period degrees of freedom of Pluto), as well as the fundamental frequencies associated with the motion of the Jovian planets. The two new fundamental frequencies must be chosen arbitrarily since there is no adequate long-period theory of Pluto to serve as a guide; the semianalytic theory of Nacozy and Diehl (1978) is overaveraged and has only one degree of freedom. By analogy with the secular perturbation theory of the other planets, we choose the new fundamental frequencies from the  $h - k$  and  $p - q$  spectra (rather than, say, the spectra of the argument of perihelion). Figure 8 shows a greatly expanded view of the very low-frequency portion of the  $h$  spectrum computed with the chirp  $z$ -transform algorithm. We choose the first fundamental frequency  $p_1$  to be the frequency of the circulation of the ascending node and the circulation of the longitude of perihelion. (These two frequencies are equal because of the libration of the argument of perihelion.) The largest peak in Fig. 8, labeled  $R$ , has

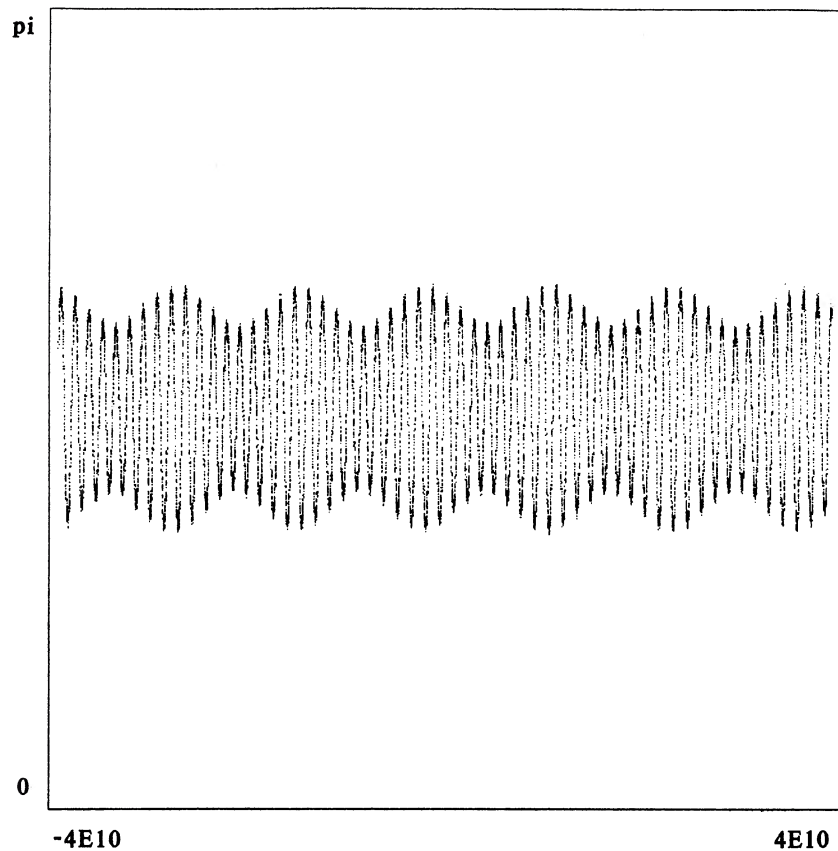


FIG. 4. The argument of perihelion  $\omega$  of Pluto for 214 Myr. The abscissa is time measured in days. The 3.80 Myr libration is amplitude modulated with a 34 Myr period.

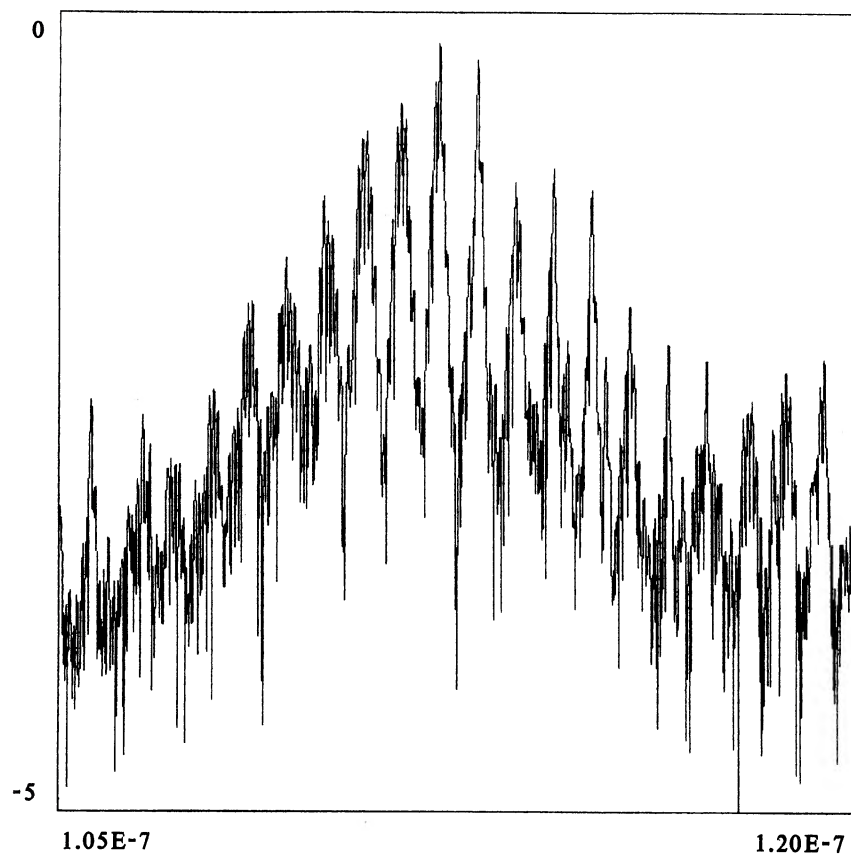


FIG. 5. Expanded view of the power spectrum of the resonant argument  $3\lambda_{\text{Pluto}} - 2\lambda_{\text{Neptune}} - \pi_{\text{Pluto}}$  of Pluto around the region where the 20 000 yr libration is aliased. In this case the aliased lines are reflected once through the Nyquist frequency,  $1.25 \times 10^{-7} \text{ day}^{-1}$ . The cluster of peaks is centered on the 19 857 yr line. The elements of the cluster are separated by the frequency corresponding to the 3.69 Myr circulation of the ascending node. This pattern is characteristic of narrowband frequency modulation. Note the unusually noisy appearance of this spectrum.

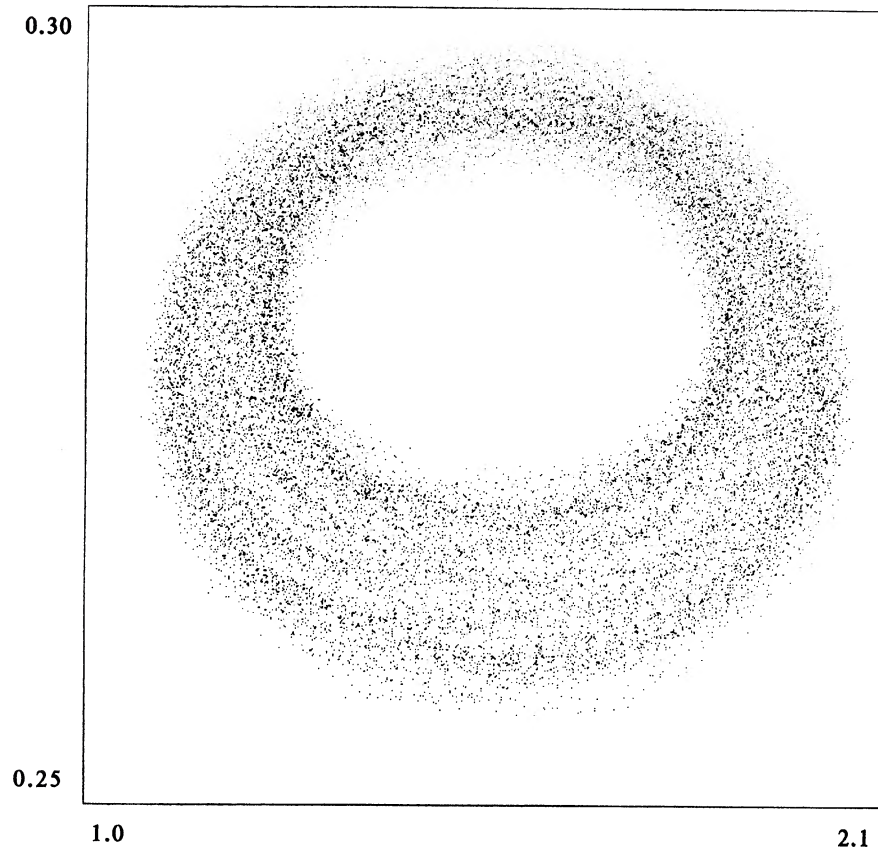


FIG. 6. The inclination of Pluto to the invariable plane, on the ordinate, is plotted against the argument of perihelion, on the abscissa. Angles are measured in radians. The argument of perihelion librates about  $\pi/2$ . The 34 Myr modulation produces the thickness of the band.

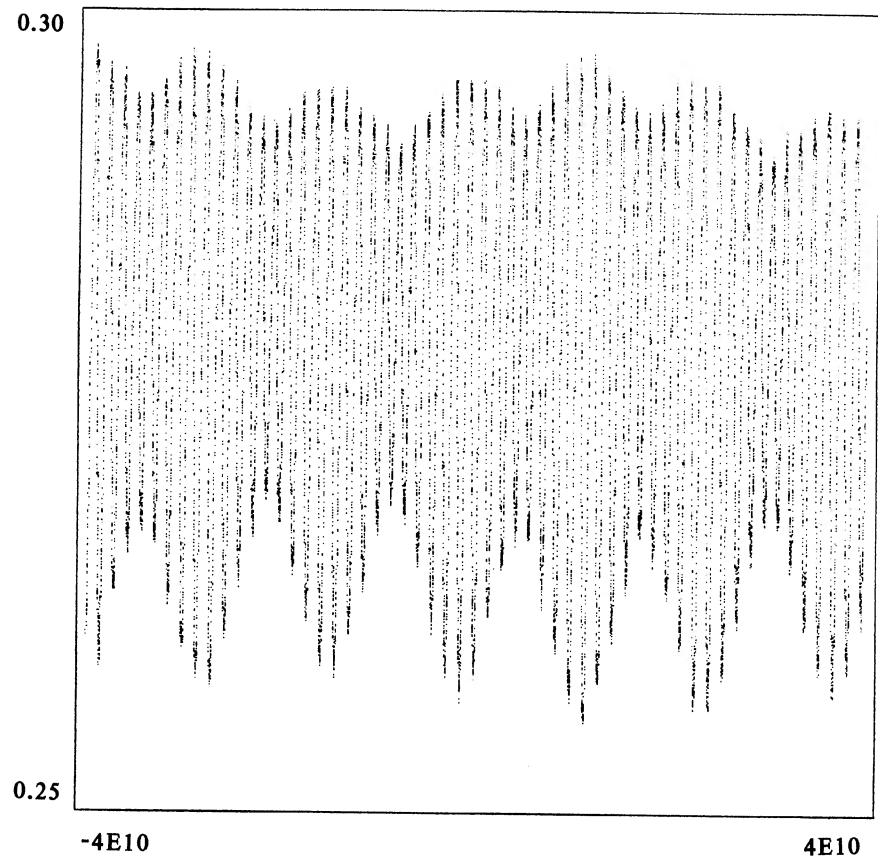


FIG. 7. Inclination of Pluto for 214 Myr. Besides the 34 Myr modulation of the 3.80 Myr oscillation, there is evidence for much longer period variations (or perhaps a secular drift).

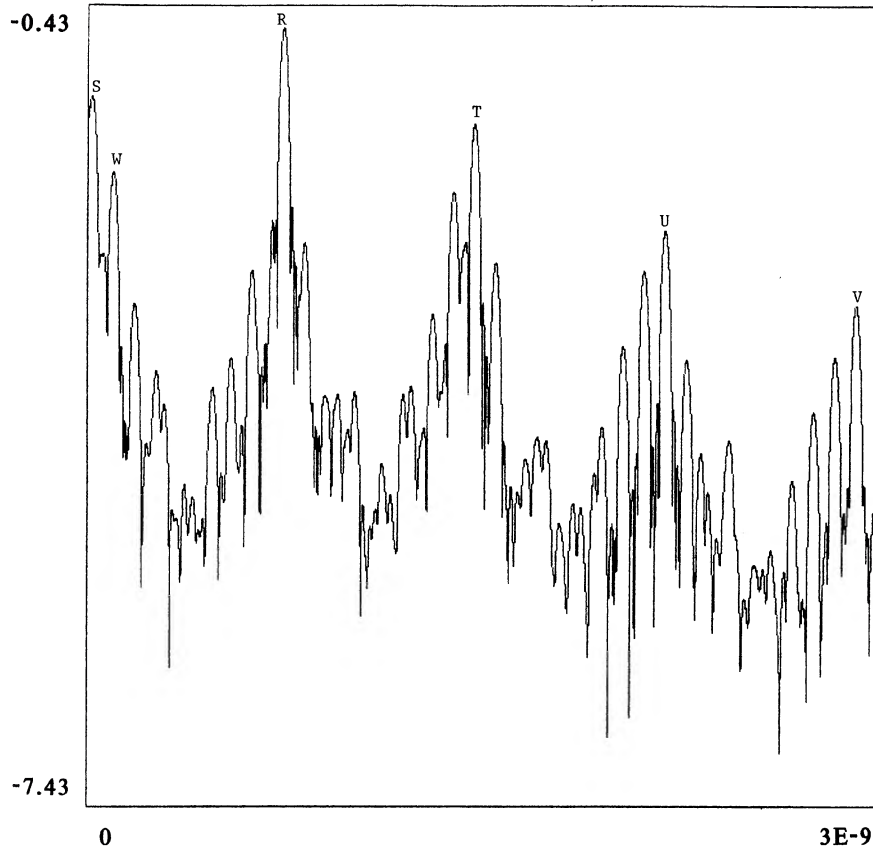


FIG. 8. Highly expanded view of the low-frequency end of the power spectrum of Pluto's  $h$ . The main peak  $R$  is  $p_1$ , the 3.69 Myr circulation of the ascending node and the longitude of perihelion. Line  $W$  is the  $p_2$  line. The peak  $T$  is the  $g_8$  line. Note the regular progression of peaks; the lines  $S$ ,  $R$ ,  $T$ ,  $U$ , and  $V$  are all separated by the same frequency. Line  $S$  has a period near 137 Myr.

the frequency  $p_1$ . A suitable choice for the second fundamental frequency is less clear. We choose  $p_2$  to be the frequency of the line marked  $W$ , which is the largest line in the long-period portion of the  $h - k$  and  $p - q$  spectra that cannot be explained as a combination of the fundamental lines previously chosen.

A summary of the main long-period lines and their relationships is given in Table IV. The rightmost peak in Pluto's  $h$ , labeled  $V$ , has a period near 943 000 yr. The largest peak  $R$  has the frequency  $p_1$ , which corresponds to a period of 3.69 Myr. The second largest line  $S$  represents the long period that is visible in the time-domain  $h$  plot shown in Fig. 9. The third largest line  $T$  is the  $g_8$  line. Numerically, the frequency of line  $S$  appears to be  $2p_1 - g_8$ . Thus the frequency of the circulation of the node  $p_1$  is nearly commensurate with the

fundamental frequency  $g_8$ . Perhaps the commensurability accounts for the strength of the very long-period variations. This near commensurability could have significant consequences for the long-term stability of Pluto.

The commensurability of  $g_8$  with  $p_1$  is an accidental property of Pluto's orbit. We have tried a variety of "Plutos" with nearby initial conditions. We have varied the initial inclination by  $\pm 5^\circ$  without changing the other elements, and we have tried various values for the argument of perihelion between 0 and  $\pi/2$ , keeping the amplitude of the libration of the resonant argument constant by varying the initial semi-major axis. The observed commensurability between  $g_8$  with  $p_1$  does not exist for nearby initial conditions.

The strongest components in the eccentricity should be simple differences of the frequencies of components of

TABLE IV. Dominant Pluto lines in  $h - k$  and  $p - q$ . Amplitudes are represented by their common logarithms.

Line	Identity	Period yr	Frequency day <sup>-1</sup>	$h - k$	$p - q$
S	$2*p_1 - g_8$	1.37e8	-2.0e-11	-1.36	-2.42
W	$p_2$	2.75e7	-9.95e-11	-1.88	-2.86
R	$p_1$	3.69e6	-7.413e-10	-0.63	-0.86
T	$g_8$	1.87e6	-1.462e-9	-1.47	-2.63
U	$2*g_8 - p_1$	1.25e6	?2.184e-9	-2.41	-3.30
V	$3*g_8 - 2*p_1$	9.41e5	-2.904e-9	-3.05	-3.57

Note: The ? in the frequency of line U indicates that the sign of the frequency could not be determined because the phases were ill defined.

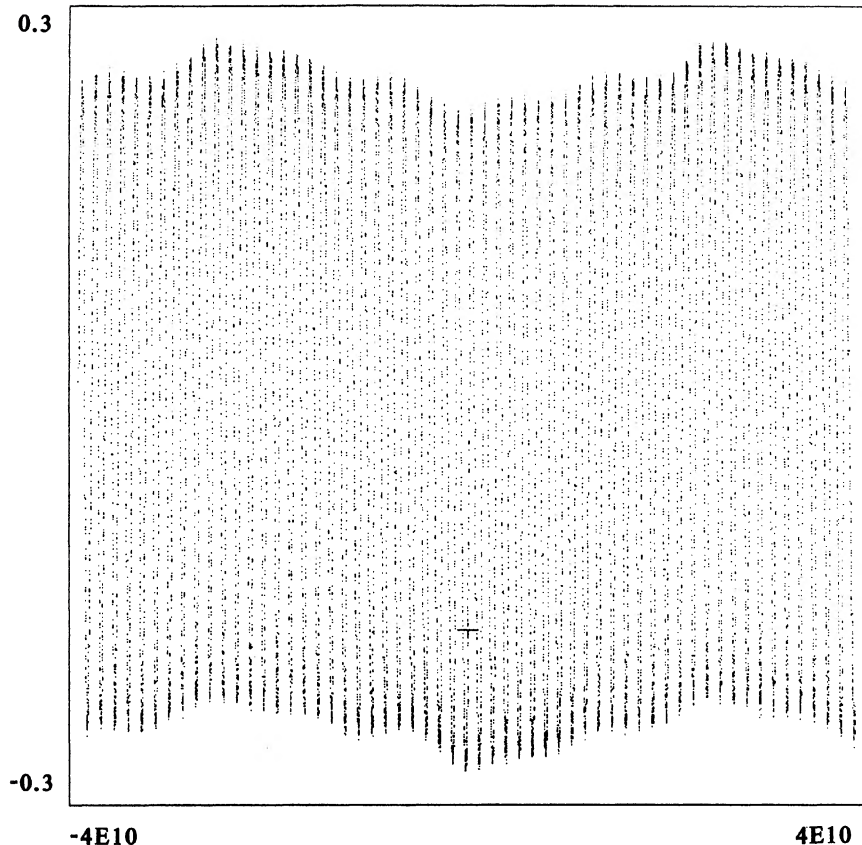


FIG. 9.  $h$  of Pluto for 214 Myr. The basic oscillation is the 3.69 Myr  $p_1$  circulation of the ascending node and longitude of perihelion. The 27 Myr  $p_2$  oscillation and the 137 Myr  $2p_1-g_8$  oscillation are evident. The small cross indicates the value of  $h$  at the current epoch.

$h - k$ . Inclination lines should be formed in a similar way from lines in  $p - q$ . In addition, frequencies of smaller lines may contain sums of frequencies of  $h - k$  or  $p - q$  lines and other even combinations of these lines. Indeed, the main lines in Pluto's  $e$ ,  $i$ , and  $\omega$  are formed in this way. Table V shows the formation of several of the largest lines.

An objective measure of the qualitative character of a solution of a set of differential equations is the Lyapunov characteristic exponent. A positive exponent indicates exponential divergence of neighboring trajectories; a zero exponent indicates quasiperiodic behavior. The maximum Lyapunov exponent can be estimated by computing the divergence of two nearby trajectories and plotting  $\log \gamma = \log [\ln(d(t)/d(t_0))/(t - t_0)]$  versus  $\log(t - t_0)$ , where  $d(t)$  is the phase-space distance between the particles at time  $t$ , and  $t_0$  is the initial time. For chaotic trajectories  $\log \gamma$  will approach the logarithm of the Lyapunov exponent, while for quasiperiodic trajectories  $\log \gamma$  versus  $\log t$  will follow a line with slope  $-1$ . In any finite computation we can only give an estimate

of this quantity which is, strictly speaking, only defined in the infinite time limit. Figure 10 shows the results of our computation of the Lyapunov exponent. Despite the odd long-period wanderings of Pluto's  $i$  and  $h$ , there is no objective evidence that Pluto, or the solar system as a whole, is chaotic. For a 110 Myr integration, the Lyapunov exponent of the solar system is estimated to be less than  $10^{-6.8}$ /yr. We have experimented with some other test particles with initial conditions close to the initial conditions for Pluto. Some of these were clearly chaotic, yet they did not have a close encounter with another planet for a full 110 Myr integration. We will report on these in another paper.

#### CONCLUSIONS

Our integrations support our prejudice that the solar system is quite stable over geologically significant time periods.

Our integrations yield a model for the long-period variations of the elements of the outer planets that is significantly more accurate than the best analytic solutions available to date. In particular, we find contributions to the variations that are not in Bretagnon's model that are larger than all but seven of his approximately 200 corrections to the Lagrange solution. Surprisingly, Brouwer and van Woerkom's estimate of the  $f_6$  frequency is more accurate than Bretagnon's. By further integration experiments we have verified that this discrepancy is not due to the effects of the inner planets. In fact, in the system of the Jovian planets alone, in the vicinity of the  $f_6$  line there are large high-order contributions that are neglected in the analytic theory. This suggests that a very high-order theory is necessary to get an accurate determination of the  $f_6$  frequency by analytic means.

TABLE V. Pluto frequencies in  $e$ ,  $i$ , and  $\omega$ . Amplitudes are represented by their common logarithms. We did not measure the signs of the frequencies of their lines.

Line	Identity	Period yr	Frequency day <sup>-1</sup>	$e$	$i$	$\omega$
L	$p_2-2*p_1+g_8$	3.44e7	7.94e-11	-3.4	-2.7	-2.2
M	$p_1-p_2$	4.27e6	6.418e-10	-2.3	-2.4	-1.0
N	$g_8-p_1$	3.798e6	7.2116e-10	-1.7	-1.8	-4.2
O	$3*p_1-p_2-2*g_8$	3.419e6	8.008e-10	-2.9	-3.0	-1.7

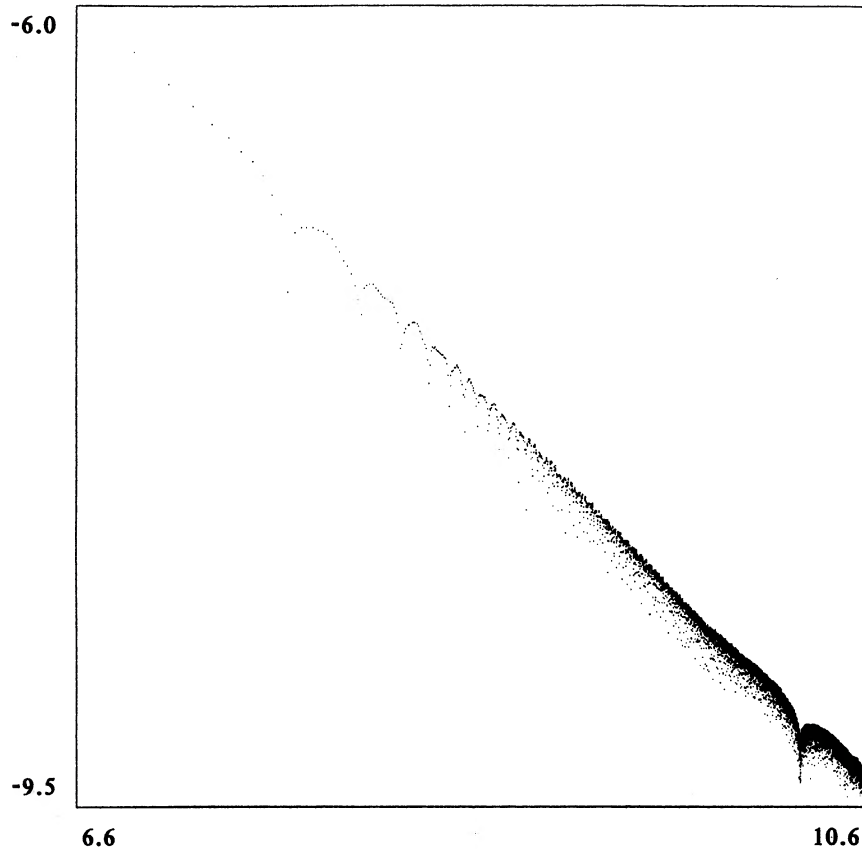


FIG. 10. The comparison of neighboring trajectories for Pluto shows no sign of a positive Lyapunov exponent. The abscissa is the common logarithm of the time since the start, in days, and the ordinate is the common logarithm of  $\gamma$ , measured in  $\text{day}^{-1}$ . The maximum Lyapunov exponent is apparently less than  $10^{-6.8} \text{ yr}^{-1}$ .

We do not know the sensitivity of our results to small variations in the masses of the planets or the initial conditions. This is an ideal problem for investigation with a highly vectorized supercomputer where many solar system models could be run simultaneously.

In any case, conclusions depending on the analytic theory must be reconsidered in the light of our findings, especially those that depend on the exact frequency of the  $f_6$  line. For example, the frequencies determine the positions of the secular resonances that in turn determine the positions of various gaps in the asteroid belt and the inner edge of the asteroid belt. Because Williams and Faulkner (1981) use the Brouwer and van Woerkom frequencies to compute the secular resonance positions, their conclusions are not substantially modified—at zero inclination, the position of the  $f_6$  secular resonance is shifted outward by only 0.02 AU from the position computed by Williams and Faulkner.

The Milankovich hypothesis is that long-term climate variations on Earth are partially caused by variations in the insolation. The insolation is itself a function of the orbital elements of Earth and the orientation of its rotation axis. Berger (1976) has used Bretagnon's model in an evaluation of the Milankovich hypothesis. However, a 7% difference in the value of the  $f_6$  frequency will cause the phase of that contribution to be inverted after only 300 000 yr. On the other hand, the contribution of the  $f_6$  line to the eccentricity of Earth's orbit is only about 1/6 of the largest contribution. In any case, this work must be rechecked.

We have observed extremely long-period variations in the orbital elements of Pluto. The eccentricity, inclination, and argument of perihelion of Pluto are modulated with a 34

Myr period. Since the long-period motion of Pluto has two degrees of freedom (corresponding to the two independent resonant arguments) the appearance of an additional fundamental frequency ( $p_2$  at 27 Myr) is to be expected. The approximately 137 Myr variation we see in  $h_{\text{Pluto}}$  is more surprising. It indicates an accidental commensurability between the secular frequency  $g_8$  and the frequency of the circulation of the node  $p_1$ . Perhaps this is important. While chaotic behavior of Pluto could have occurred in the two degree of freedom long-period problem, on the time scale of our integrations, we see no evidence of such instability. The maximum Lyapunov characteristic exponent appears to be less than  $10^{-6.8} \text{ yr}^{-1}$ . However, with the 20 000 yr mean-motion resonance and the 3.796 Myr  $\omega$  libration resonance, this commensurability between  $g_8$  and  $p_1$  may provide just what is needed to make the orbit of Pluto chaotic over much longer time scales. Perhaps we will observe instability in our billion year integrations.

The authors would like to thank Scott Tremaine for his help and for his encouragement of this project. We are grateful to the Hewlett-Packard Company, Cupertino Integrated Circuits Organization, for supplying the special floating-point adder and multiplier chips that made this project possible, and to Chuck Seitz of Caltech for helping with the construction of the Orrery. We thank Richard Feynman for his help with numerical analysis. We also thank A. Miliani, A. Nobili, K. Fox, and C. Murray for helpful criticism and encouragement. We also want to thank the referee, J. G. Williams, whose comments led to a substantial improve-

ment of this paper. This research was supported in part by the NASA Planetary Geology and Geophysics Program under Grant NAGW-706. The authors are listed in alphabetical order.

## APPENDIX

In this Appendix, we supply invariable-frame center-of-mass coordinates and velocities of the outer planets listed at approximately 11 Myr intervals ( $4.0 \times 10^9$  days) for approximately 110 Myr. For each epoch, the  $x$ ,  $y$ , and  $z$  coordinates of the position and the velocity of each body are given. Positions are in AU, velocities are in AU/day. Caution: This table is printed with a large number of significant places. This is not intended to indicate the accuracy of these numbers. After 110 Myr the integration error in the position of Jupiter is a large fraction of an orbit. Many places are

offered solely for the purpose of precise reproduction and testing of our results. We integrate Pluto as a zero-mass test particle, for the other planets we use the CHO masses:

Body	Reciprocal mass
Sun	1.0
Jupiter	1047.355
Saturn	3501.6
Uranus	22869
Neptune	19314
Pluto	zero mass

The sum of the masses of the inner planets is  $0.597682 \times 10^{-5}$ . The Gaussian constant is 0.01720209895. Our initial conditions are for J. D. 2430000.5, copied from CHO:

J. D. 2430000.5

Sun			
	-4.06428567034226E-003	-6.08813756435987E-003	-1.66162304225834E-006
	6.69048890636161E-006	-6.33922479583593E-006	-3.13202145590767E-009
Jupiter			
	3.40546614227466E+000	3.62978190075864E+000	3.42386261766577E-002
	-5.59797969310664E-003	5.51815399480116E-003	-2.66711392865591E-006
Saturn			
	6.60801554403466E+000	6.38084674585064E+000	-1.36145963724542E-001
	-4.17354020307064E-003	3.99723751748116E-003	1.67206320571441E-005
Uranus			
	1.11636331405597E+001	1.60373479057256E+001	3.61783279369958E-001
	-3.25884806151064E-003	2.06438412905916E-003	-2.17699042180559E-005
Neptune			
	-3.01777243405203E+001	1.91155314998064E+000	-1.53887595621042E-001
	-2.17471785045538E-004	-3.11361111025884E-003	3.58344705491441E-005
Pluto			
	-2.13858977531573E+001	3.20719104739886E+001	2.49245689556096E+000
	-1.76936577252484E-003	-2.06720938381724E-003	6.58091931493844E-004

J. D. 4002430000.5

Sun			
	3.48223323133294E-003	-5.14286882438496E-003	6.42295997953432E-005
	6.99036259576250E-006	-6.68635026091231E-007	-1.84571827079439E-008
Jupiter			
	1.61746471832055E+000	4.95217444751191E+000	-1.88332403665657E-002
	-7.08766744678321E-003	2.52010658679173E-003	3.53463052614887E-005
Saturn			
	-1.00147212070865E+001	2.34829982895445E+000	-1.04707804806302E-001
	-1.06650965907352E-003	-5.03824327277739E-003	-6.43693947258976E-005
Uranus			
	-1.40377335981219E+001	-1.21373363763877E+001	3.13477343821166E-002
	2.48032164285927E-003	-3.21481640139462E-003	7.65553703275585E-005
Neptune			
	-2.99890268409148E+001	5.30636341320454E+000	-3.42175281320721E-001
	-5.22984243478207E-004	-3.05370005372625E-003	-4.93621278591275E-006
Pluto			
	4.45173202040767E+001	4.64963741941285E+000	-1.11244716244025E+001
	1.37872077689202E-004	2.27755980086148E-003	-3.71785740399728E-004

J. D. 8002430000.5

Sun			
	1.55869198405522E-004	-3.18403735475778E-003	1.08836667678877E-005
	5.39160393755459E-006	3.43231235257224E-008	7.35556929980973E-008
Jupiter			
	-5.44729539898946E-001	5.41799893231953E+000	1.13950632794564E-002
	-7.16675004958545E-003	-5.94418785410185E-004	-5.08047879625351E-005

Saturn  
 3.54564152580684E+000 -8.74621730590543E+000 2.06135684103364E-002  
 5.32043382196174E-003 1.84433478081138E-003 -8.19257759180138E-005

Uranus  
 1.95630741804694E+001 2.71780478978726E+000 -2.93842766872591E-001  
 -6.50823674708960E-004 3.76013227655692E-003 4.02799045695946E-006

Neptune  
 -2.90434891624838E+001 7.53163376490776E+000 -2.85883308656771E-001  
 -7.70500814382826E-004 -3.04993242053356E-003 -3.53038934787746E-005

Pluto  
 1.75152554330301E+001 -2.82660062106951E+001 2.07127824781659E+000  
 2.96906833418316E-003 9.51086077045478E-004 -7.39161649624750E-004

J.D. 12002430000.5

Sun  
 2.16760593763746E-003 -7.2222306693325E-003 -3.15449540367761E-005  
 7.61520042957956E-006 2.10694058046252E-006 -2.63984885742415E-008

Jupiter  
 -1.91624116724281E+000 4.90690123135316E+000 -1.21294100709737E-002  
 -6.75468231460021E-003 -3.10003052639295E-003 4.40061982227405E-005

Saturn  
 6.76825525524820E+000 6.62825051289516E+000 1.36821733133484E-001  
 -3.82866204482741E-003 4.10289639223501E-003 -3.84208074824303E-005

Uranus  
 -1.94371585954775E+001 7.12459915758657E-001 -5.67184312770713E-002  
 -1.44364395609248E-004 -3.87282609534166E-003 -7.26422112585187E-005

Neptune  
 -2.74440706887983E+001 1.18415484883449E+001 1.26158495520580E-001  
 -1.27960784828791E-003 -2.88665654819439E-003 -2.83733014319321E-005

Pluto  
 -1.20764756309941E+001 3.86602941387661E+001 -7.51165871252173E+000  
 -2.20618557580004E-003 -1.27298474290349E-003 5.96558570088588E-004

J.D. 16002430000.5

Sun  
 6.50963831183654E-003 -4.78476579136663E-003 -4.19212523656333E-005  
 5.53227733444709E-006 7.13351656818888E-006 3.47104548933087E-008

Jupiter  
 -3.74865453594555E+000 3.34109578830954E+000 -1.93001385459315E-002  
 -5.13292664282553E-003 -5.86304160956797E-003 -5.20870372647430E-005

Saturn  
 -8.21572501979340E+000 3.67351862497295E+000 9.12755874981280E-002  
 -2.14461713364704E-003 -5.48880502566165E-003 5.49049636095309E-005

Uranus  
 1.69016814347972E+001 -6.56637329418294E+000 3.20323467366284E-001  
 1.55074386127937E-003 3.85196557535484E-003 -1.16586357761641E-005

Neptune  
 -2.55573979756374E+001 1.60830378404650E+001 3.91597005357944E-001  
 -1.67656082030944E-003 -2.63696428483002E-003 -2.87482304537816E-006

Pluto  
 4.40762053188755E+001 4.24164281996522E+000 -5.14997629409785E+000  
 2.16842046524218E-004 2.30927079918678E-003 -6.46238501654341E-004

J.D. 20002430000.5

Sun  
 5.52370658890758E-003 -5.85828041842782E-004 -1.70676598693163E-005  
 1.60116973753634E-006 6.69992534492122E-006 -4.13311417283429E-008

Jupiter  
 -4.68031337944589E+000 1.82726427188393E+000 1.42744898234868E-002  
 -2.94440784864176E-003 -7.21603288517162E-003 9.60218582533074E-006

Saturn  
 2.50191641873675E+000 -9.81704959722601E+000 -8.58645594555737E-003  
 5.02899732471168E-003 1.45797094588450E-003 9.84259551882108E-005

Uranus  
 -1.19983255302817E+001 1.65889069176537E+001 -3.28798095835417E-002  
 -2.97537197582829E-003 -2.15413786455044E-003 6.70903408470075E-005

Neptune  
 -2.40433351247357E+001 1.77539929885424E+001 1.41544150864033E-001  
 -1.85403597610088E-003 -2.55670198245339E-003 2.16475730225097E-005

Pluto  
 5.11389786559684E+000 -2.95852108067399E+001 8.28422936812740E+000  
 3.38713829798115E-003 9.15457760686447E-005 -1.37072741219185E-004

J.D. 24002430000.5

Sun  
 4.23664486163340E-003 -1.88623421298253E-003 9.64322707745441E-005  
 1.04376519239950E-006 5.98832048345574E-006 -3.68770969502140E-009

Jupiter  
 -5.32551359019271E+000 -2.93572213974529E-001 -4.29858168175026E-002  
 1.91013028503073E-005 -7.34592249237651E-003 -1.20568232770501E-005

Saturn  
 6.57076550576522E+000 6.92672495058619E+000 -1.03157253655313E-001  
 -3.95466139790090E-003 3.91577086101041E-003 4.78674567586954E-005

Uranus  
 3.42352483017958E+000 -1.83566500192271E+001 -3.16498458287528E-001  
 3.96713411447061E-003 7.46490274236667E-004 -3.30515613730046E-006

Neptune  
 -2.27545827594062E+001 1.913737464447912E+001 -2.33526787235125E-001  
 -2.04910439860953E-003 -2.42379178407079E-003 3.23273419266869E-005

Pluto  
 -4.03030205035373E+000 4.56782699971212E+001 -1.39212971213227E+001  
 -2.18952952349382E-003 -2.46591037673138E-004 1.58565647969970E-005

J.D. 28002430000.5

Sun  
 8.61197183605486E-003 -1.52191606336924E-003 2.12686089274339E-005  
 -1.00069705146846E-006 8.23053690598849E-006 3.22486369592157E-008

Jupiter  
 -5.27028919471399E+000 -1.31712395740664E+000 3.50776423487000E-002  
 1.89759344379601E-003 -6.94558423909119E-003 -1.71911380994973E-005

Saturn  
 -9.19626163474942E+000 2.60359970651520E+000 -1.32824607238309E-001  
 -1.78889454915172E-003 -5.26201577273889E-003 -4.39064061915997E-005

Uranus  
 8.69431097112419E-001 1.88507814395373E+001 -5.80567744546339E-003  
 -3.99280596022371E-003 1.22497797829261E-004 -7.51185536205692E-005

Neptune  
 -1.91537795884695E+001 2.33971674397009E+001 -3.20117401527937E-001  
 -2.42620431301525E-003 -1.96325215017069E-003 -2.17896265864682E-007

Pluto  
 2.37852118021572E+001 3.33316621708725E+001 -7.57648285684333E+000  
 -1.73123452178467E-003 1.80924976864970E-003 -6.57807229934771E-004

J.D. 32002430000.5

Sun  
 5.29517287415151E-003 4.50016974301791E-003 2.77183378213456E-005  
 -5.43457528625935E-006 6.11118866899664E-006 1.09626231979361E-008

Jupiter  
 -4.53094682765573E+000 -2.59611647359337E+000 -3.40764660633709E-002  
 3.89595304220610E-003 -6.40679989059352E-003 1.76809675487063E-005

Saturn  
 3.42671456683762E-001 -8.88440201648099E+000 -1.16080876733586E-002  
 5.94415364753047E-003 5.07707314115164E-004 -9.02250227034650E-005

Uranus  
 -5.93630690949659E+000 -1.91425604330546E+001 3.31078321450774E-001  
 3.53469430286160E-003 -1.27562427623985E-003 2.58817114609627E-006

Neptune  
 -1.55935849988451E+001 2.61231437761550E+001 -1.22560187959805E-001  
 -2.65201199183582E-003 -1.60914612769619E-003 -4.23093606662130E-005  
 Pluto  
 -3.27389770115819E+001 -2.08180336667930E+001 1.03183955458065E+000  
 1.95516788080658E-003 -1.82862231122927E-003 7.44435957572349E-004

J.D. 36002430000.5

Sun  
 1.10078140151875E-003 3.21060447564082E-005 -6.11493629868046E-005  
 -4.32406444740262E-006 3.81882503575273E-006 3.75951684870714E-008  
 Jupiter  
 -3.57482684181278E+000 -3.51331815945287E+000 2.05248440092848E-002  
 5.66517105961183E-003 -5.38977455078203E-003 -2.33897660975661E-005  
 Saturn  
 8.47989031555101E+000 5.26572254021547E+000 1.34774368525477E-001  
 -2.91879138364036E-003 4.44601095405309E-003 -5.76677127079669E-005  
 Uranus  
 1.51072149156528E+001 1.07814360852296E+001 -5.99154409177859E-002  
 -2.52004191424286E-003 3.18265868462124E-003 7.21662908916507E-005  
 Neptune  
 -1.48699767282820E+001 2.60124717855582E+001 1.09756641971781E-001  
 -2.72679500617084E-003 -1.57686341901427E-003 -3.76593469208598E-005  
 Pluto  
 -3.8542487653777E+001 2.81416712262605E+001 -1.26275918035680E+001  
 -1.36225740673516E-003 -1.62482411805361E-003 1.19699042013392E-004

J.D. 40002430000.5

Sun  
 5.11103294604065E-003 1.87723534619512E-003 -3.33343443425492E-005  
 -5.92783401638197E-006 4.18682312303781E-006 -6.53614916331504E-008  
 Jupiter  
 -1.59975525403686E+000 -4.76955151543362E+000 -1.80081565191346E-003  
 7.24902527595051E-003 -2.84299406489444E-003 5.61190869237519E-005  
 Saturn  
 -7.80989146903828E+000 5.77368422097477E+000 1.20832014723732E-001  
 -3.22962602132352E-003 -4.41342438075074E-003 4.06869096922042E-005  
 Uranus  
 -1.70580418054650E+001 -9.27395055298758E+000 -3.88300602525694E-001  
 1.81253346708702E-003 -3.43384541827910E-003 -6.48353508887316E-007  
 Neptune  
 -1.17311815271961E+001 2.76773207866022E+001 3.38479266746031E-001  
 -2.90342966186623E-003 -1.19441376100762E-003 3.65013585190970E-006  
 Pluto  
 2.99156240156959E+001 5.71207786015946E+000 5.32189283403254E+000  
 6.92050814781919E-006 3.36730530918591E-003 -5.77927353015376E-004

#### REFERENCES

- Anolik, M. V., Krassinsky, B. A., and Pius, L. J. (1969). *Trudy Inst. Theor. Astron., Leningrad* **14**, 3.  
 Applegate, J. F., Douglas, M. R., Gürsel, Y., Hunter, P., Seitz, C., and Sussman, G. J. (1985). *IEEE Trans. Comput.* **C34**, 822.  
 Arnold, V. I. (1961). *Russian Math. Surveys* **18**, 85.  
 Berger, A. L. (1976). *Astron. Astrophys.* **51**, 127.  
 Bretagnon, P. (1974). *Astron. Astrophys.* **30**, 141.  
 Brouwer, D. (1937). *Astron. J.* **46**, 149.  
 Brouwer, D. (1966). In *The theory of orbits in the solar system and in stellar systems*, edited by G. Contopolous (Academic, London and New York).  
 Brouwer, D., and Clemence, G. M. (1961). *Methods of celestial mechanics* (Academic, New York).  
 Brouwer, D., and van Woerkom, A. J. J. (1950). *Astron. Papers Am. Ephemeris XII*, II.  
 Cohen, C. J., and Hubbard, E. C. (1965). *Astron. J.* **70**, 10.  
 Cohen, C. J., Hubbard, E. C., and Oesterwinter, C. (1973). *Astron. Papers Am. Ephemeris XXII*, I.  
 Duriez, L. (1979). "Approche d'une théorie générale planétaire en variables elliptiques héliocentriques", unpublished thesis, Lille, France.  
 Kinoshita, H., and Nakai, H. (1984). *Celest. Mech.* **34**, 203.  
 Milani, A., and Nobili, A. M. (1985). *Celest. Mech.* **35**, 269.  
 Nacozy, P. E., and Diehl, R. E. (1978). *Astron. J.* **83**, 522.  
 Rabiner, L. R., Schafer, R. W., and Rader, C. M. (1969). *Bell System Tech. J.* **48**, 1249.  
 Schubart, J. (1964). *Smithson. Astrophys. Obs. Spec. Rep. No.* 149.  
 Williams, J. G., and Benson, G. S. (1971). *Astron. J.* **76**, 167.  
 Williams, J. G. and Faulkner, J. (1981). *Icarus* **46**, 390.  
 Wisdom, J. (1982). *Astron. J.* **87**, 577.  
 Wisdom, J. (1983). *Icarus* **56**, 51.